

## Poster Setup and Presentation Times

**Poster Presentation Times**

*(Please plan to attend your posters during the following times)*

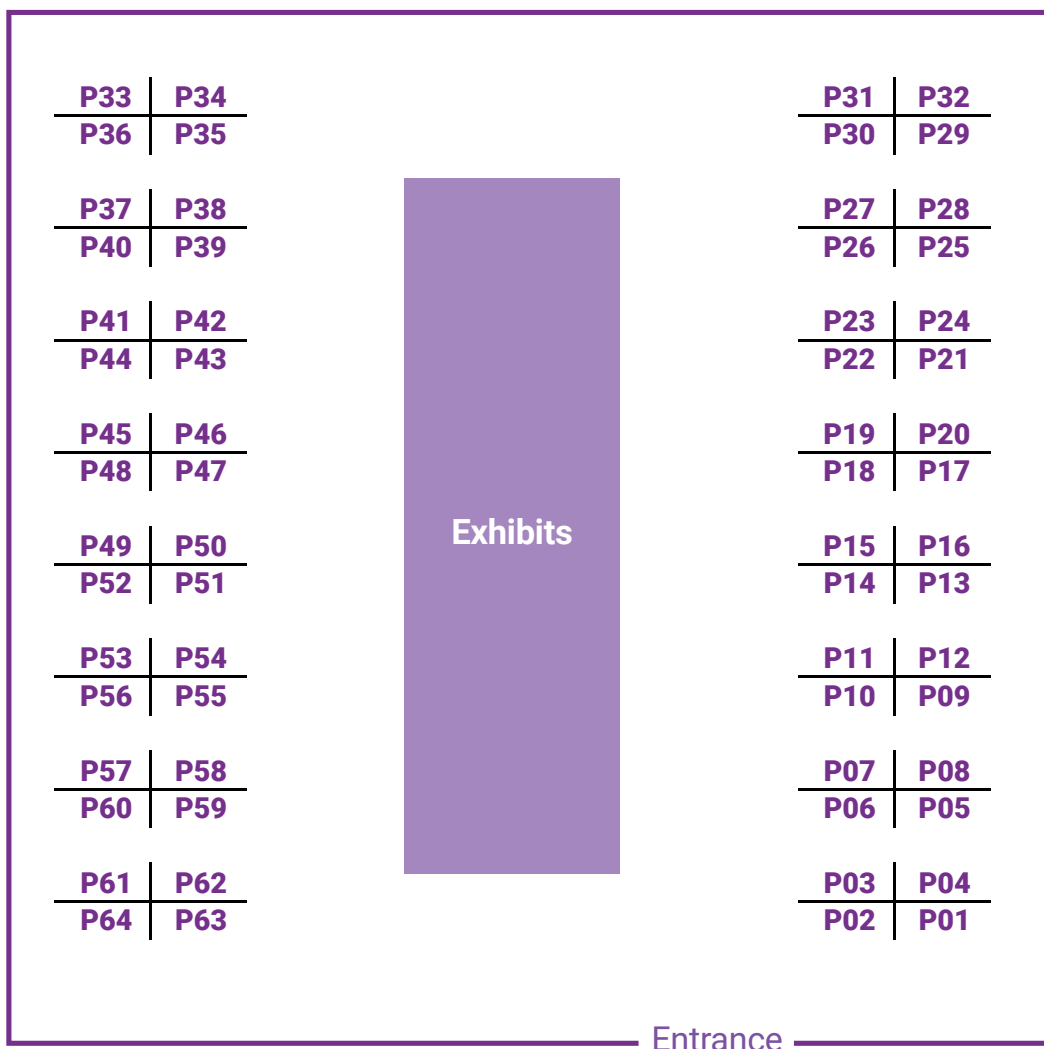
Sunday, June 16 (Welcome Reception) ..... 6:00 PM–6:30 PM  
 Monday, June 17 ..... 10:30 AM–11:00 AM and 3:05 PM–3:35 PM  
 Tuesday, June 18 ..... 9:40 AM–10:10 AM and 3:25 PM–3:55 PM  
 Wednesday, June 19 ..... 9:45 AM–10:15 AM

**Poster Setup**

Sunday, June 16 ..... 12:00 PM–5:00 PM

**Poster Teardown**

Wednesday, June 19 ..... 1:00 PM–2:00 PM  
 If your poster is not removed before 2:00 PM, it will be removed and placed near the Registration Desk for pickup.



## Poster Presentation Index

### Poster Categories

Young Investigator Award Candidate..... P01–P14  
 General Pathology/Toxicologic Pathology..... P15–P29, P63  
 New Technologies ..... P30–P43

Systemic/Organ-Specific Toxicologic Pathology..... P44–P55  
 Biomarkers ..... P56  
 Oncology/Carcinogenesis..... P57–P62

**P01 Atopic Dermatitis Promotes Food Allergy through Intestinal Remodeling and Metabolic Perturbances**

*Katelin L. Davis, Estefania Claudio-Etienne, Benjamin Schwarz, Derron A. Alves, Lashawna Leak, Karen Laky, Pamela A. Frischmeyer-Guerrero*

**P02 Role of *Staphylococcus aureus* Superantigens in Atopic Dermatitis Pathogenesis**

*Laine E. Feller, Sabrina N. Kline, Jing Zhang, Yu Wang, Nathan K. Archer*

**P03 Time-of-Day Difference in Inflammatory Response and Circadian Clock Gene Expression in Acutely Ozone-Exposed Mice**

*Rekha K.C., Ishita Choudhary, Yogesh Saini*

**P04 Mapping the Dynamics of Research Trends in Environmental Toxicology: A Twenty-Year Scientometric Analysis**

*Vanitha Thurairasu*

**P05 Local Tissue Response to a C-X-C Motif Chemokine Ligand 12 (CXCL12) Therapy for Fecal Incontinence in a Rabbit Model**

*Hannah Ruetten, Shannon Lankford, Nicholas Edenhoffer, Gopal Badlani, James K. Williams*

**P06 A C-X-C Motif Chemokine Ligand 12 (CXCL12) Therapy for Underactive Bladder in a Rat Model**

*Hannah Ruetten, Shannon Lankford, Gopal Badlani, James K. Williams*

**P07 *Pseudomonas aeruginosa*-Derived Volatile Organic Compounds Activate Aryl Hydrocarbon Receptor Signaling and Polarize toward M1 Macrophage, Neutrophils, and Type 17 Immune Responses That Favor Mucus Hypersecretion in Diseased Lungs**

*Shanny H. Kuo, Jaishree Sharma, Som Nanjappa, Gee Lau*

**P08 Characterizing the Role of N<sup>6</sup>-methyladenosine (m<sup>6</sup>A) in the Oncogenic Retrovirus HTLV-1**

*Emily M. King, Amanda Midkiff, Amanda R. Panfil*

**P09 SREBP1 Drives Lipogenesis and Autophagy to Promote Cell Survival through Fatty Acid Oxidation in Hypoxic Triple-Negative Breast Cancer Cells**

*Jae-Ha Jung, Yeseul Yang, Goeun Choi, Hyun-ki Hong, Habin Jung, Yongbaek Kim*

**P10 Paired Single-Cell RNA and T Cell Receptor Sequencing Revealed Clonal Expansion and Differential Gene Expression of the Mutant IL-7R-RasGRP1-Driven Leukemia**

*Steven Hsu, Gisele Olinto Libanio Rodrigues, Julie Hixon, Wenqing Li, Scott K. Durum*

**P11 A Novel TGF $\beta$  Pathway Reporter Mouse Reveals New Insights into Therapeutic Safety and Tumorigenesis**

*Zachary Millman, Yu-an Yang, Christina Stuelten, Hibret Adissu, Jennifer Dwyer, Mark Simpson, Lalage Wakefield*

**P12 Prenatal Exposure to Cadmium Alters Macrophage Subpopulations in Mouse Placentas**

*Brianna C. Ames, Shine Wang, Danielle L. Kozlosky, Sean Stratton, Carol R. Gardner, Brian T. Buckley, Debra L. Laskin, Lauren M. Aleksunes*

**P13 1-Trichloromethyl-1,2,3,4-tetrahydro-beta-carboline (TaClo)-Induced Developmental Toxicity and Neurotoxicity in the Zebrafish Model following the Early-Life Exposure**

*Ji-Hang Yin, Katharine Horzmann*

**P14 Effects of Soy Isoflavones on Hormone Secretion in the Male Gonad**

*Kristen G. Hoehler, Benson T. Akingbemi*

**P15 Characterization of 3D Models of Human Uterine Endometrium for Use in Evaluating the Role of Environmental Toxicants in Endometrial Cancer**

*Jingli Liu, Linda Yu, Lysandra Castro, Yitang Yan, Darlene Dixon*

**P16 Intrahepatic Cholangiocarcinoma with Pulmonary Metastasis in a Rhesus Macaque (*Macaca mulatta*)**

*Addressa Varella Gonsioroski, Mayra Tsoi, Meredith Leigh Cronin, Nicholas Vetter*

**P17 MRI and Histological Measures of Myelination Are Correlated in a Rat Model of BPA Neurotoxicity**

*Bradley C. Wright, Joel P. Levoy, Elizabeth M. Fugate, Diana M. Lindquist, Alex Edmondson*

**P18 Neuropathology Evaluation of Olney Lesions in Regulatory Drug Development Toxicology Studies**

*Deepa B. Rao, William H. Jordan, David G. Hall*

**P19 Spontaneous Splenic Hemangiosarcoma in a Young Sprague-Dawley Rat**

*Fei Zhou, Xixing Zhao, Yu Ma, Tiansheng Zhou, Yuanyuan Duan, Hegen Dai, Xihua Wang, Yinghong Hu*

**P20 Poster Withdrawn**

**P21 Anticoagulant Rodenticide Toxicity in Three Red-Tailed Hawks (*Buteo jamaicensis*) from Northeastern Massachusetts**

*Jiashi Feng, Julia Lombardo, Felix Valles Feliciano, Erin Hutchings, Brittany Rasche*

**P22 Exploring the Potential of Natural Compound 6'-Hydroxy Justicidin B as a Therapeutic Agent against COVID-19: In**

## **Vitro and In Vivo Nonclinical Efficacy and Toxicity Studies following Good Laboratory Practice Standards**

*Byoung-Seok Lee, Min Heui Yoo, Han Young Eom, Kang-Hyun Han, Joung-Wook Seo, Junguk Choi, Jihyun Jeon, Sangho Lee, Seungtaek Kim, Yong-Bum Kim*

## **P23 Assessment of 6'-Hydroxy Justicidin B as a Potential Therapeutic for COVID-19: Nonclinical Efficacy and Good Laboratory Practice (GLP) Toxicity Studies In Vitro and In Vivo**

*Ji-Seok Han, Min Heui Yoo, Tae-Yang Jung, Heejin Park, Eun Mee Lee, Min Seng Jang, Seng-Min Back, Yunha Hwang, Jihyun Youm, Yong-Bum Kim*

## **P24 Pyogranulomatous Inflammation Associated with an Extended-Release Buprenorphine Injection Formulation in Rabbits**

*Lori E. Bedient, Eleana R. Sosnowski, L. Michele Wilkinson*

## **P25 Presumptive Red Maple Leaf Toxicosis in a Horse**

*Luan C. Henker, Danyue Kang, Thainá Lunardon, Rachel Neto*

## **P26 Histologic Assessment of Inflammation in Mouse Models of Inflammatory Bowel Disease Using Digital Pathology**

*Morgan Maisel, Sean Graham, Katie Malley, Caroline Morel, Brendan Oakes, Andrew McKnight, Dinesh Bangari*

## **P27 Assessment and Validation of Deep Learning Algorithms in Identifying Early Chronic Progressive Nephropathy Changes**

*Priyanka Thakur, David Cunefare, Charan Ganta, Cynthia Willson, Allison C. Boone, Katherine Allen-Moyer, Keith Shockley, Eli Ney, Ronald Herbert, Mark Cesta*

## **P28 Early Deaths of Rabbits Resulting from Potential Pregnancy Toxemia in a Developmental Toxicity Study**

*Rongrong Li, Tiansheng Zhou, Rong Xu, Lin Zhu, Lei Wang, Xixing Zhao*

## **P29 Common Spontaneous Neoplastic Findings in Tg.rash2 Mice Used in Nonclinical Research Studies**

*Victoria A. Laast, Alok K. Sharma*

## **P30 Whole Brain Assessment of Myelin in a Rat Model of Bisphenol-A Exposure**

*Alex Edmondson, Bradley Wright, Joel Levoy, Beth Fugate, Diana Lindquist*

## **P31 Performance Evaluation of Standard vs. Automated AI-Based Image Analysis of Hepatic Necrosis in KO vs. WT Mice Infected with Listeria Monocytogenes**

*Charan Ganta, David Cunefare, Priyanka Thakur, Prashant Rai, Eli Ney, Michael Fessler, Ronald Herbert*

## **P32 Enabling Rat Bone Marrow Cell Lineage Identification in H&E Whole Slide Images Using Multiple IHC-Guided Deep Learning Models**

*Edgar A. Rios Piedra, Marco Tecilla, Ines Berenguer Veiga, Kerstin Hahn, Pierre Maliver, Jeff Eastham, Adeyemi O. Adedeji, Shari Lau, Miriam Baca, Ruth Sullivan*

## **P33 The Development and Optimization of a Novel Image Analysis Solution for the Detection of Low-Grade Thyroid Follicular Cell Hypertrophy in Rats**

*James Baily, Stuart Naylor, James Alibhai, Elizabeth McInnes*

## **P34 Unraveling the Complexity of Injection Site Reactions Using Spatial Transcriptomics, Proteomics & Histopathology in an Ex Vivo Human Skin Model**

*Deidre A. Dalmás, Ali Ebrahimi, Chavon Williams, LiJun Zhou, Kelly Diegel, Thilo Werner, Susan Laffan, H. Christian Eberl, Kate Annunziato*

## **P35 Single-Cell Finding Detection and Quantification for Cellular-Level Microscopic Findings Using Deep-Learning Approaches**

*Hope Williams, Jogile Kuklyte, Laoise Lord Bissett, Sarah Marcu, Esther Crouch, Lise Bertrand, Daniel Rudmann, Pierre Moulin*

## **P36 Development of AI Classifiers and Integration into a Commercially Available Decision Support Tool for Toxicologic Pathology**

*Jogile Kuklyte, Laoise Lord Bissett, Hope Williams, Eoghan Keany, Esther Crouch, Lise Bertrand, Daniel Rudmann, Pierre Moulin*

## **P37 13-Week Repeat-Dose Rat Intrathecal Toxicity Studies for Four MOE ASOs Intended for the Treatment of Nano-Rare Neurological Disease**

*Lisa Berman-Booty, Christine Hoffmaster, Julie Veyssiere, Claudine Tremblay, Erica Twitchell, Nicole Hamelin, Luc Chouinard, Catherine Parisien, Julie Douville, Scott Henry*

## **P38 Absolute Quantitation vs. Semi-Quantitative Analysis of Expression of Biomarkers Using Image Analysis Software**

*Sasmita Mishra, Tyler Peat, Victoria Arndt, Susan Lynk, Steve Van Adestine, Pamela Blackshear*

## **P39 Deep Learning-Based Method for Anatomical Subsite-Wise Evaluation of Single Cell Necrosis and Vacuolation of Neuron/Nerve Fiber of CNS Toxicity in Rats**

*Taishi Shimazaki, Yuzo Yasui, Kyotaka Muta, Naohito Yamada, Amogh Mohanty, Aashay Tinaikar, Rohit Garg, Tijo Thomas, Toshiyuki Shoda*

## **P40 Deep Learning Solution for the Automated Assessment of the Rodent Thymus**

*Rajesh Ugalmugle, Deb Tokarz, Dev Kumar Das, Gunjan Deotale, Tijo Thomas, Uttara Joshi*

## **P41 AI-Based Approach for Quantifying and Grading Bile Duct Hyperplasia in Mice**

*Ingeborg M. Langohr, Dayananda Siddappa Thimmanahalli, Nathan Pate, Dinesh S. Bangari, Dev Kumar Das, Kuldeep Gautam, Arshad Kazi, Tijo Thomas, Uttara Joshi, Rajesh Ugalmugle*

## **P42 Development and Evaluation of HALO and HALO AI Image Analysis Tools for Quantitative Histopathology Scoring of Lung Pathology in Experimental Tuberculosis Infections of Rhesus Macaques**

*Vinay Shivanna, Olga Gonzalez, Edward J. Dick, Jr.*

**P43 Solving the Reference Pathologist Paradox in Machine Learning Development for Histology Scoring**

*Thomas Forest, Sabu Kuruvilla, Binod Jacob, Nagaraja Muniappa, Takayuki Tsuchiya, Raymond Gonzalez, Malini Roy, Raghav Amaravadi, Geetank Raipuria, Nitin Singhal*

**P44 Congenital Thyroid Dysplasia in C57BL/6NTac Due to LINE Transposition into Thyroglobulin Gene**

*Thomas Forest, Wendy Bailey, Bart Smits, Zoltan Erdos, John Gaspar, Warren Glaab, Sabu Kuruvilla, Pamela Lane, Thomas Rosahl, Douglas Thudium, Jingzhou Wang, Melissa MacGowan, Heather Multari, Christine Cumo, Adam Navis*

**P45 Safety Assessment of Repeated Intra-Articular Injections of pMPCylated Liposomes in Rat Models for Knee Osteoarthritis Therapy**

*Yuval Ramot, Noam Kronfeld, Michal Steiner, Eric D. Lee, Ronit Goldberg, Sabrinal Jahn, Abraham Nyska*

**P46 Effects of the Pharmacological YAP-TEADs Inhibitor Verteporfin in Preovulatory Bovine Granulosa Cells Viability**

*Esdras Correa dos Santos, Christopher Price, Gustavo Zamberlam*

**P47 A SARS-CoV2 mRNA Vaccine Candidate (CUK3-1/LNP128) Induces Reversible Bone Marrow Suppression in ICR Mice**

*Jae-Hun Ahn, Na-Young Lee, Hee-Jin Bae, Euna Kwon, Gyochang Keum, Jae-Hwan Nam, Byeong-Cheol Kang*

**P48 Development-Limiting Toxicity Associated with a Dual Targeting Bispecific T-Cell Engager in a 28-Day Nonhuman Primate Toxicology Study**

*Joan H. Lane, Rhian Prunicki, Rodolfovan Yabut, William Siska, Christine Mollica*

**P49 Use of Virtual Control Groups in Nonhuman Primate Ocular Nonclinical Toxicity Studies**

*Oliver C. Turner, Clare Thomas, Christopher Hayden, Johann Mueller, Helen Booler*

**P50 Background Findings of Infrequently Examined Bones in Beagle Dogs**

*Phaedra I. Cole, Agathe Bédard, Sara Tonissen*

**P51 Retrospective Review of Histopathology Findings in Beagle Dogs in Powder Inhalation Toxicology Studies**

*Predrag Novakovic, Joseph Younan, William Lee, Kevin McNally, Lev Kolodzieyski, Stephen Groom*

**P52 Procedure-Related, Artifact, and Spontaneous Background Microscopic Findings in Eyes from African Green Monkeys (*Chlorocebus sabaeus*) Used in Ocular Toxicology Studies**

*Rahul B. Dange, Jennifer Cann, Richard Bouffard, Melissa Miles, Emily Ramirez, Nadine Swierzawski, Matthew Lawrence*

**P53 Procedure-Related, Artifact, and Spontaneous Background Microscopic Findings in Central Nervous System and Dorsal Root Ganglion from African Green Monkeys (*Chlorocebus sabaeus*) Used in Neurotoxicology Studies**

*Rahul B. Dange, Jennifer Cann, Richard Bouffard, Melissa Miles, Emily Ramirez, Golnaz Jalalahmadi, Matthew Lawrence*

**P54 Pathology Associated with Human CAR T Cell in NSG Mice: A Retrospective Review**

*Renata M. Mammona, Alessandra Piersigilli, Ileana C. Miranda*

**P55 Investigation of Human and Bovine Thrombin-Effects on Cynomolgus Monkey Platelets and Evaluation of a Monoclonal Antibody Specific for Human Thrombin Receptor**

*Florence M. Poitout-Belissent, Anthony Pincon, Weizhen Wu, Katherine Larocque, Lori Morton, Dan Chalothorn*

**P56 Investigation of Compound-Related Effects on Fibrinolysis with a Microplate Turbidimetric Fibrinolytic Assay**

*Anthony Pincon, Florence M. Poitout-Belissent, Tetyana Redko, Marc-Olivier Pepin, Dorothy Flood, Tom J. Parry*

**P57 Evaluation of the Translational Relevance of Rat Mammary Tumors to Human Breast Cancer Using Immunophenotypic Characterization**

*Allison C. Boone, Morgan Hernandez, Heather Jensen, David Cunefare, Charan Ganta, Keith Shockley, Cynthia Rider, Ronald Herbert, Robert Sills, Arun Pandiri*

**P58 Rodent Tumors from  $\alpha$ -Pinene Exposure Harbor Unique Mutation Signatures and Enriched Mutational Motifs**

*Arun Pandiri, Jianying Li, Ashley Brooks, Dmitry Gordenin, Leszek Klimczak, Ella Gunady, Thai-Vu Ton, Cynthia Rider, Ronald Herbert, Robert Sills, Jian-Liang Li, David Adams*

**P59 Spontaneous Neoplasms in the Ovary of Mice from Carcinogenicity Studies**

*Marcia E. Pereira Bacares, Loudon D. Yantis*

**P60 Histopathological Characterization of Immune Checkpoint Inhibitor Toxicities in a Humanized Immune System Mouse Model**

*Michael J. Goedken, Sarah Asby, Julie Lang, Jordi Lanis, Zander Kostka-Newman, Kristina Larsen, Scott Tilden, Roberta Pelanda, Xia Wen, Lauren M. Aleksunes, Melanie S. Joy*

**P61 Preclinical Dog Model of Focal Prostate Cancer: Pathology and Novel Theranostics**

*Nathan K. Hoggard, Gopalakrishnan Ramamurthy, Felipe Berg, Xinning Wang, Eric T. Hosnik, Matthew Joseph, Reena Shakya, Dario Palmieri, Krishan Kumar, Richard M. James, Arijit Ghosh, Dong Luo, Michael V. Knopp, Agata A. Exner, James P. Basilion, Michael F. Tweedle, Thomas J. Rosol*

**P62 Evaluation of the Immune Landscape in a Rat Colon Tumor Model Using Imaging Mass Cytometry**

*Xuying Zhang, Allison Boone, Ricardo Cortes, Kevin Katen, Carl Bortner, Arun Pandiri*

**P63 INHAND: International Harmonization of Nomenclature and Diagnostic Criteria for Lesions—An Update—2024**

*Emily K. Meseck, Mark F. Cesta, Stacey Fossey, Victoria Laast, John L. Vahle, Alys Bradley, Matt Jacobsen, Ute Bach, Rupert Kellner, Thomas Nolte, Susanne Rittinghausen, Shim-mo Hayashi, Takanori Harada, Junko Satou, Katsuhiko Yoshizawa*

# Abstracts

## P01 Atopic Dermatitis Promotes Food Allergy Through Intestinal Remodeling and Metabolic Perturbances

*Katelin L. Davis*<sup>1,2</sup>, *Estefania Claudio-Etienne*<sup>1</sup>, *Benjamin Schwarz*<sup>1</sup>, *Derron A Alves*<sup>1</sup>, *Lashawna Leak*<sup>1</sup>, *Karen Laky*<sup>1</sup>, *Pamela A. Frischmeyer-Guerrero*<sup>1</sup>

<sup>1</sup>National Institute of Allergy and Infectious Diseases, Bethesda, MD, USA. <sup>2</sup>Purdue University, West Lafayette, IN, USA.

### Abstract

One of the strongest risk factors for food allergy (FA) development is atopic dermatitis (AD). Nearly half of children with AD will go on to have FA; an epidemiologic phenomenon known as the atopic march. Current models propose that food antigen exposure through the disrupted skin barrier of AD lesions leads to food specific IgE production and sensitization. Beyond a role in sensitization, little is known about how AD predisposes the immune system to allergic disease in distant organs. To address this question, MC903 was applied to the ear of mice to induce AD followed by ovalbumin to promote food sensitization. Mice developed ovalbumin-specific IgE antibodies and anaphylaxed to ovalbumin upon challenge, similar to infants with FA. Thus, we validated our mouse model of the atopic march. AD, alone, induced changes in the intestinal cellular composition and metabolome. AD mice had increased numbers of goblet cells, tuft cells, and intraepithelial mucosal mast cells. Within the lamina propria we detected increased numbers of GATA3+ Tregs and less IL-10 producing macrophages. T lymphocytes within the mesenteric lymph nodes produced more IL-4 upon stimulation. LC-MS analysis of the plasma, small intestine, and feces revealed that AD mice had increased levels of unconjugated bile acids in their feces, decreased levels of tryptophan and cyclooxygenase dependent metabolites in their intestine, and alterations in circulating and intestinal neurotransmitters. These findings indicate that AD induces a proinflammatory, type 2 skewed environment in the small intestine which may interfere with oral tolerance and predispose AD patients to FA.

## P02 Role of *Staphylococcus aureus* Superantigens in Atopic Dermatitis Pathogenesis

*Laine E. Feller*, *Sabrina N. Kline*, *Jing Zhang*, *Yu Wang*, *Nathan K. Archer*

Johns Hopkins University, Baltimore, MD, USA.

### Abstract

Atopic dermatitis (AD) is a chronic, relapsing, itchy, and inflammatory skin disorder that affects 25% of children and 7-10% of adults. AD pathogenesis involves a complex interaction of epidermal barrier defects, immune dysregulation, and alterations in the skin microbiome including abundant colonization by *Staphylococcus aureus* (SA). While SA burden is associated with AD development and severity, how SA interacts with host cells to drive AD progression is incompletely understood. Superantigens (SAGs) are a major staphylococcal virulence factor and potent T cell mitogen due to their ability to circumvent the classical antigen presentation pathway. Instead, these toxins non-specifically cross-link MHC class II and CD4+ T cell receptors outside the peptide-binding site leading to oligoclonal T cell activation. Using our mouse model of AD, wherein epicutaneous exposure to SA for 7 days induces AD-like skin inflammation, we have found that staphylococcal SAGs, particularly Toxic Shock Syndrome Toxin (TSST), are involved in AD pathogenesis. C57BL/6J mice colonized by SA deficient in TSST demonstrate markedly reduced epidermal thickness, serum IgE production, and myeloid and lymphoid infiltration into the skin compared to those colonized by TSST-producing SA. Notably, these results phenocopied when performed in transgenic mice expressing human MHC class II molecules (HLA-DR4 mice), suggesting that this is a relevant and translatable finding for human AD. These results indicated a role for SA-derived SAGs in orchestrating AD pathogenesis, with downstream implications for therapeutics and vaccines targeting SAGs for the treatment of AD and potentially other inflammatory skin diseases complicated by SA skin colonization.

## P03 Time-of-Day Difference in Inflammatory Response and Circadian Clock Gene Expression in Acutely Ozone-Exposed Mice

*Rekha K C, Ishita Choudhary, Yogesh Saini*  
North Carolina State University, Raleigh, NC, USA.

### Abstract

Exposure to ground level ozone induces lung injury, inflammatory responses, and altered lung function. The key mediators of inflammation such as circulating immune cells and cytokines exhibit circadian rhythms and oscillate in a 24-hour cycle. However, time-of-day dependent inflammatory responses in ozone-exposed mice is unclear. Eight weeks old C57BL/6J mice (n=10 in each group) were exposed to 1.5 ppm ozone for 4 hours at two different time points of the day: 6-10 am and 6-10 pm, with appropriate filtered air (FA)-exposed control group. Alterations in the circadian gene expression in lung tissues were assessed using RT-PCR. Exaggerated inflammatory response and lung injury were observed in ozone-exposed mice compared to FA-exposed mice. Compared to mice exposed to ozone in morning time, immune cell recruitment and epithelial injury indicated by increase in total cell count and total protein concentration in the bronchoalveolar lavage fluid (BALF); and expression of found in inflammatory zone protein 1 (FIZZ1), an M2 macrophage activation marker in lung tissues were significantly higher in mice exposed to ozone in the nighttime. Inflammatory mediators, including KC, MIP1a, Eotaxin and IL-5 also tended to be higher in the BALF of mice exposed to ozone at nighttime than exposed to ozone in morning time. Ozone exposure at nighttime significantly decreased Circadian gene (*Per1* and *Cry1*) expression. These findings suggest that exposure of mice to ozone at nighttime induces profound inflammatory responses and dysregulation of circadian gene expression making mice more sensitive to ozone induced lung injury.

## P04 Mapping the Dynamics of Research Trends in Environmental Toxicology: A Twenty-Year Scientometric Analysis

*Vanitha Thurairasu*  
The National University of Malaysia, Kuala Lumpur, Malaysia.

### Abstract

**Introduction:** Environmental health and toxicology research is crucial for understanding the impacts of environmental factors on human health and ecosystems. It has evolved significantly due to technological advances. However, the absence of in-depth analysis of research trends could result in a disproportionate allocation of attention and resources, favoring certain areas while neglecting others.

**Objective:** This study aims to trace the development of environmental health and toxicology research from 2003 to 2023, highlighting trends, global research contributions, and emerging topics, offering a comprehensive overview of the field's evolution.

**Methodology:** Using Scopus and Web of Science, this study analyzed publications in environmental health and toxicology from 2008 to 2023. Bibliometric and scientometric techniques such as citation analysis and keyword mapping were applied to map global research trends comprehensively.

**Results:** The study showed a significant increase in interdisciplinary research, particularly on emerging pollutants and their effects, with leading contributions from the United States, Europe, China, and India, indicating global research efforts. Key emerging themes included climate change, nanomaterial risks and new analytical technologies. However, research from the developing countries was notably underrepresented.

**Conclusions:** This paper reveals significant growth in environmental health and toxicology research, highlighting increased interdisciplinary and international collaboration. It provides a crucial framework, prioritizing future policy-making, while calling for focused efforts in underrepresented regions to ensure equitable resource allocation and improved infrastructure.

**Impact Statement:** The evaluation of two decades of environmental health and toxicology research emphasizes the urgent need for focused and equitable efforts in tackling emerging environmental challenges.

## P05 Local Tissue Response to a C-X-C Motif Chemokine Ligand 12 (CXCL12) Therapy for Fecal Incontinence in a Rabbit Model

*Hannah Ruetten*<sup>1,2</sup>, *Shannon Lankford*<sup>1</sup>, *Nicholas Edenhoffer*<sup>1</sup>, *Gopal Badlani*<sup>3,4</sup>, *James K. Williams*<sup>1</sup>

<sup>1</sup>Wake Forest Institute for Regenerative Medicine, Winston-Salem, NC, USA. <sup>2</sup>Wake Forest School of Medicine, Winston-Salem, NC, USA. <sup>3</sup>Wake Forest Baptist Medical Center, Winston-Salem, NC, USA. <sup>4</sup>VA Medical Center, Salisbury, NC, USA.

### Abstract

Obstetric anal sphincter injuries often result in muscle and nerve damage leading to fibrosis and loss of muscle tone. CXCL12 is a chemokine known to recruit progenitor cells. We investigated if local injection of human recombinant CXCL12 would reduce fibrosis, restore muscle content, vascularization, and innervation, and recruit progenitor cells at injury site. Study groups: control, injured/treated (treated), and injured/no treatment (untreated) (four adult female rabbits each). Injury: 5x10mm section of sphincter removed. Treatment: 200ng CXCL12 at six weeks. Euthanasia: 12 weeks. FFPE sphincter tissue collected. Collagen was assessed using picrosirius red. Immunohistochemistry for MYH1, UCHL1, PECAM, and CD34 was performed. Statistics: ANOVA or a Kruskal-Wallis test,  $p < 0.05$  significant. Images (1 /animal, 10x, injury site) were analyzed and study group was masked. MYH1 images were assessed for distinct muscle layering and organization fibers within layers. Compared to controls, untreated had indistinct or absent muscle layering in the sphincter ( $p < 0.05$ ), circumferential and inner longitudinal layers were disorganized ( $p < 0.05$ ), and lower percentage area stained positive for MYH1 ( $p < 0.01$ ). In untreated, collagen fiber density was increased ( $p < 0.05$ ) and more cells stained positive for CD34 in the muscle ( $p = 0.03$  to  $< 0.01$ ), compared to treated and controls. PGP9.5 and CD31 and cells staining positive for CD34 within the rectal mucosa/submucosae were similar amongst all groups ( $p = 0.97$ ,  $p = 0.93$ , and  $p = 0.80$ ). Local injection of CXCL12 reduces post-injury fibrosis and results in restoration of muscle content. Based upon our evaluation, local injection of CXCL12 appears to be a promising new treatment for post-parturient anal incontinence.

## P06 A C-X-C Motif Chemokine Ligand 12 (CXCL12) Therapy for Underactive Bladder in a Rat Model

*Hannah Ruetten*<sup>1,2</sup>, *Shannon Lankford*<sup>1</sup>, *Gopal Badlani*<sup>3,4</sup>, *James K. Williams*<sup>1</sup>

<sup>1</sup>Wake Forest Institute for Regenerative Medicine, Winston-Salem, NC, USA. <sup>2</sup>Wake Forest School of Medicine, Winston-Salem, NC, USA. <sup>3</sup>Wake Forest Baptist Medical Center, Winston-Salem, NC, USA. <sup>4</sup>VA Medical Center, Salisbury, NC, USA.

### Abstract

Treatment for under active bladder includes surgical removal of obstruction and palliative therapeutics. Even when obstruction is removed, detrusor doesn't fully recover. We investigate if local injection of human recombinant CXCL12, alone or in combination with surgical release, can restore detrusor function. Study design: two phases using adult male rats ( $n = 4-7$  /group). Phase one: controls, and obstructed/no treatment for 6 weeks, 9 weeks, and 12 weeks. Phase two: CXCL12, surgical release and CXCL12/surgical release, all rats obstructed, treatment 6 weeks, endpoint 12 weeks, void spot assay performed at 5 time points. Obstruction: silk ligature around urethra to cause partial obstruction. Treatments: CXCL12, intra-detrusor injection of 200ng; surgical release, ligature removed. Cystometry was performed immediately prior to euthanasia in all. Control data from phase one were used for phase two. In phase one, bladder compliance (infused volume/ leak point pressure) was significantly reduced in the 12 week group compared to week 9 and control ( $p = 0.01$ ,  $p = 0.03$ ). In phase two, bladder compliance was significantly reduced in all treatment groups compared to control ( $p = 0.004$ ,  $p = 0.02$ ,  $p = 0.002$ ). Analysis of additional functional parameters, and bladder tissue are ongoing. Phase one, we were able to induce outlet obstruction resulting in reduced bladder compliance at 12 weeks. Phase two, none of our treatments restored bladder compliance; data analysis is ongoing to determine if there are any additional signs of detrusor improvement. Our model responds similar to in humans, surgical release of the obstruction did not restore bladder compliance, making this an ideal model for ongoing studies.

**P07 *Pseudomonas aeruginosa*-Derived Volatile Organic Compounds Activate Aryl Hydrocarbon Receptor Signaling and Polarize toward M1 Macrophage, Neutrophils, and Type 17 Immune Responses that Favor Mucus Hypersecretion in Diseased Lungs**

*Shanny H. Kuo, Jaishree Sharma, Som Nanjappa, Gee Lau*  
University of Illinois at Urbana-Champaign, Champaign, IL, USA.

**Abstract**

**Introduction:** The aryl hydrocarbon receptor (AhR) has emerged as a regulator of mucosal barrier function, influencing immune responsiveness in lung by modulating mucin and cytokine production. AhR is known to bind small molecules derived from the microorganisms, pollutants, diets, and metabolism. Highly expressed in immunocytes, AhR signaling plays roles in integrating the effects of the environmental stimuli and immune response. We have previously demonstrated *Pseudomonas aeruginosa* (PA)-derived volatile organic compounds (VOCs) cause airway mucus hypersecretion via AhR-mediated FOXA2 degradation that leads to MUC5AC/MUC5B overexpression and goblet cell metaplasia. We hypothesize the PA-derived VOCs may activate immune cell subsets contributing to disease pathogenesis and mucus hypersecretion. **Methods:** C57BL6 mice (6-week-old, n=8, equal sexes) were exposed to VOCs once daily for 3 weeks. Single cells from BAL and lavaged lungs were stained with specific antibodies and analyzed by flow cytometry. Lung tissue was evaluated by PAS staining and immunohistochemistry (MUC5AC, MUC5B, and FOXA2). **Results:** Flow cytometry revealed predominantly M1 macrophages (58%), neutrophils (11%), and IL-17A<sup>+</sup>secreting T lymphocytes (12%). In C57BL/6 mice, selective depletion of either macrophages (via clodronate liposome) or neutrophils (via anti-mouse Ly6G) decreased mucin production and restored FOXA2 expression in VOCs-exposed mouse airways. Similarly, IL-17a<sup>-/-</sup> mice lacking IL-17A showed attenuated mucin production and restored FOXA2 activity following VOCs exposure. **Conclusions:** VOCs polarize toward M1 macrophages, neutrophils, and type 17 proinflammatory responses in mouse airway that favor mucus hypersecretion. **Impact Statement:** Our data accentuate the immunomodulatory role of VOCs in mediating mucus hypersecretion, highlighting the multifarious impact of VOCs during infection.

**P08 Characterizing the Role of N-6-methyladenosine (m6A) in the Oncogenic Retrovirus HTLV-1**

*Emily M. King, Amanda Midkiff, Amanda R. Panfil*  
The Ohio State University, Columbus, OH, USA.

**Abstract**

Human T-cell leukemia virus type 1 (HTLV-1) is an oncogenic retrovirus that infects 5-10 million people worldwide. Approximately 10% of those infected develop disease (adult T-cell leukemia/lymphoma, myelopathy/spastic paraparesis, inflammatory disease) after a prolonged clinical latency period. Patient prognosis is poor with few therapeutic options. Viral genes *Tax* and *Hbz* are critical to viral persistence and pathogenesis. Methylation of the N6 position of adenine (m6A) is the most common post-transcriptional modification, which until now has not been documented in HTLV-1. This modification is identified by cellular reader proteins (YTHDF1-3, YTHDC1-2) that recognize m6A and regulate target gene expression. We therefore hypothesize that the m6A modification of *tax* and/or *hbz* regulates viral gene expression and subsequent viral-mediated cellular proliferation and cancer development. We performed CLIP assays and showed that both *tax* and *hbz* mRNAs contain m6A modifications and reader proteins YTHDC1 and YTHDF1 bind the viral transcripts *tax* and *hbz*. Knockdown of YTHDC1 and YTHDF1 causes a decrease in sense- (*tax*, *gag*, *env*) and antisense (*hbz*) transcripts, *Tax* protein expression, and infectious viral particle (p19) release. Furthermore, YTHDC1 promotes nuclear export of *tax* transcripts, which is dependent on m6A-modifications of the *tax* mRNA. Sites of m6A modification were mapped within the HTLV-1 genome using MeRIP-Seq. We identified 3 major enrichment peaks, the largest of which localizes to the region of the genome encoding both *Tax* and *Hbz* genes. Understanding how m6A impacts HTLV-1 pathogenesis can lead to introduction of new therapeutics through m6A-targeted therapies.

## P09 SREBP1 Drives Lipogenesis and Autophagy to Promote Cell Survival Through Fatty Acid Oxidation in Hypoxic Triple-Negative Breast Cancer Cells

*Jae-Ha Jung*<sup>1,2</sup>, *Yeseul Yang*<sup>1</sup>, *Goeun Choi*<sup>1</sup>, *Hyun-ki Hong*<sup>1</sup>, *Habin Jung*<sup>1</sup>, *Yongbaek Kim*<sup>1,3</sup>

<sup>1</sup>Laboratory of Clinical Pathology, Seoul National University, Seoul, Republic of Korea. <sup>2</sup>BK<sup>21</sup> Four Future Veterinary Medicine Leading Education and Research Center, Seoul, Republic of Korea. <sup>3</sup>Research Institute for Veterinary Science, College of Veterinary Medicine, Seoul National University, Seoul, Republic of Korea.

### Abstract

**Introduction:** Lipid reprogramming within cultured cells plays a pivotal role in their survival under hostile environments. Our objective was to delineate the effect of lipid reprogramming on cancer cells with distinct phenotypes under hypoxia. **Experimental Design:** We employed three human breast cell lines: MCF-10a (non-cancerous), MCF-7 (estrogen receptor positive), and MDA-MB-231 (triple-negative). To induce hypoxia, the cells were incubated in a hypoxia chamber set to 1% O<sub>2</sub> for 48 hours. **Methods:** Cell viability was assessed by trypan blue staining, MTT, and Annexin V-PI assays. Intracellular lipid levels were quantified using Nile red stain with immunofluorescence (IF). Autophagy was detected using LC3 antibody, Cyto-ID stain, IF, Western blotting, and flow cytometry. Fatostatin and rapamycin served as an inhibitor of sterol regulatory element-binding protein 1 (SREBP1) and an inducer of autophagy, respectively. **Results:** The cell viability showed a noteworthy elevation in MDA-MB-231 compared to MCF-10A and MCF-7. SREBP1 was found to be a central player in promoting lipogenesis and autophagy in MDA-MB-231. Conversely, cell viability declined upon SREBP1 inhibition but rebounded upon co-treatment with an autophagy inducer under hypoxia. Notably, inhibition of SREBP1 led to a downregulation of fatty acid oxidation (FAO) and ATP production. **Conclusion:** Our findings offer convincing evidence that the orchestrated lipid reprogramming by SREBP1 and autophagy under hypoxia enhance cell survival via ATP production through FAO particularly in a cell type dependent manner. **Impact statement:** Our findings also suggest that the reprogrammed lipid metabolism and subsequent autophagy could be a valuable indicator of toxicity, which warrants further studies using various toxic agents and cell lines.

## P10 Paired Single-Cell RNA and T Cell Receptor Sequencing Revealed Clonal Expansion and Differential Gene Expression of the Mutant IL-7R-RasGRP1-Driven Leukemia

*Steven Hsu*<sup>1,2,3</sup>, *Gisele Olinto Libanio Rodrigues*<sup>2</sup>, *Julie Hixon*<sup>2</sup>, *Wenqing Li*<sup>2</sup>, *Scott K. Durum*<sup>2</sup>

<sup>1</sup>Comparative Biomedical Scientist Training Program, Bethesda, MD, USA. <sup>2</sup>National Cancer Institute, Frederick, MD, USA. <sup>3</sup>Michigan State University, East Lansing, MI, USA.

### Abstract

Approximately 10% of T cell acute lymphoblastic leukemia (TALL) cases harbor mutations in the IL-7 receptor (mIL7R) that render it constitutively active; however, mIL-7R alone is insufficient to transform thymocytes. A second oncogene, such the overexpression of RasGRP1, cooperates with mIL-7R to drive leukemogenesis. Intriguingly, this mIL-7R-RasGRP1-driven leukemia expresses TCR $\beta$  (H57-597 clone) and  $\gamma\delta$  (GL3 clone) by flowcytometry. It is unclear how the addition of RasGRP1 overexpression affects gene expression to drive leukemogenesis; furthermore, how it affects T cell receptor (TCR) rearrangement to drive aberrant TCR pairing in the mIL-7R-RasGRP1-driven murine model of TALL. 10X Genomics' Chromium single cell 5' gene expression and immune profiling solutions with custom Trg (TCR $\delta$ ) and Trd (TCR $\delta$ ) primers were employed to compare gene expression and TCR rearrangement of double negative (n=2), mIL-7R-transduced (n=2), and mIL-7R-RasGRP1-transduced thymocytes (n=2). Suppression of SOCS1 ( $p=1.43 \times 10^{-55}$ ) and dominance of clones with Trbv12-2, Trbv3, and Trbv13-3 were identified in the mIL-7R-RasGRP1 group. Meanwhile, the mIL-7R group had suppression of murine IL-7R and dominance of clones with Trbc1, Trbv12-1, and Trbv4. 0.5%, 5.26%, and 5.56% of double negative, mIL-7R-transduced, and mIL-7R-RasGRP1-transduced thymocytes expressed Tra, Trb, and Trg, respective to each group. Mechanistically, SOCS1 is a key regulator of JAK-STAT pathway and acts as a negative feedback mechanism. Thus, the suppression of SOCS1 by mIL-7R-RasGRP1-driven leukemia may represent the suppression of a negative feedback mechanism and potentiation of the effects of the mIL-7R. Single-cell TCR sequencing supports the oligoclonal expansion of the mIL-7R-RasGRP1-driven leukemia and the aberrant expression of TCR $\alpha\beta\gamma$ .

## P11 A Novel TGF $\beta$ Pathway Reporter Mouse Reveals New Insights into Therapeutic Safety and Tumorigenesis

Zachary Millman<sup>1</sup>, Yu-an Yang<sup>1</sup>, Christina Stuelten<sup>1</sup>, Hibret Adissu<sup>2</sup>, Jennifer Dwyer<sup>1</sup>, Mark Simpson<sup>1</sup>, Lalage Wakefield<sup>1</sup>

<sup>1</sup>National Cancer Institute, National Institutes of Health, Bethesda, MD, USA. <sup>2</sup>Clinical Pharmacology and Safety Sciences, BioPharmaceuticals R&D, AstraZeneca, Gaithersburg, MD, USA.

### Abstract

Transforming growth factor-beta (TGF $\beta$ ) promotes tumor progression and cancer therapy resistance, making this multifunctional and biologically complex cytokine a critical therapeutic target. Consequently, TGF $\beta$  antagonists have entered early clinical trials. Our lab has developed the "Lime" mouse, a novel transgenic TGF $\beta$  pathway reporter mouse with a strong Smad3-binding element which drives GFP expression (S3>GFP) to view TGF $\beta$  signaling from whole-body to single-cell levels. This model provides a unique view of TGF $\beta$  signaling in normal mouse homeostasis. To determine which cell populations exhibited TGF $\beta$  signaling in Lime mice, a genotype-blinded, whole-body immunohistochemical survey for GFP was performed consisting of six GFP-positive reporter mice and two GFP-negative control mice, aged 6 months, with equal numbers of both sexes in each group. Endothelial cells and chondrocytes of Lime mice were immunoreactive, consistent with cardiovascular and skeletal toxicities described in pre-clinical studies with TGF $\beta$  antagonists, indicating a homeostatic role of TGF $\beta$  in these tissues. Secretory epithelial cells within multiple organs had strong immunoreactivity, suggesting an unanticipated role for TGF $\beta$  superfamily members in regulating the secretory phenotype. Furthermore, intercrossing Lime mice with MMTV-HER2/neu mice ("LimeHER2") revealed distinct spatial heterogeneity patterns in TGF $\beta$  signaling throughout the stages of tumorigenesis in GFP immunolabeled LimeHER2 mammary tumors, suggesting a spatially-specified role for TGF $\beta$  in mediating crosstalk between tumor cells and the tumor microenvironment. This novel reporter mouse will further our understanding of the cellular distribution and function of TGF $\beta$  signaling, offering fresh insights into tumorigenesis and tumor progression as well as toxicities associated with TGF $\beta$  antagonists.

## P12 Prenatal Exposure to Cadmium Alters Macrophage Subpopulations in Mouse Placentas

Brianna C. Ames, Shine Wang, Danielle L. Kozlosky, Sean Stratton, Carol R. Gardner, Brian T. Buckley, Debra L. Laskin, Lauren M. Aleksunes

Rutgers University, Piscataway, NJ, USA.

### Abstract

**Background:** Cadmium (Cd) accumulates in the placenta and has been associated with preterm birth and fetal growth restriction in rodents and humans. In humans, we observed that higher maternal exposure to Cd is associated with altered macrophage subpopulations in term placentas. Here, we assessed whether prenatal exposure of mice to CdCl<sub>2</sub> alters macrophage populations in placentas.

**Methods:** Wild-type C57BL/6CrI mice were mated overnight marking gestational day (GD) 0. On GD7, dams (n=9-10/group) received either distilled water or CdCl<sub>2</sub> (5 or 50 ppm) *ad libitum* through GD17, when tissues were collected.

**Results:** Compared to controls, dams exposed to 50 ppm CdCl<sub>2</sub> gained less weight by GD17. Circulating Cd concentrations were similar to controls in dams treated with 5 ppm CdCl<sub>2</sub> (0.27 vs. 0.50 ng/mL Cd) and elevated in dams receiving 50 ppm CdCl<sub>2</sub> (3.66 ng/mL Cd). Fetoplacental weight and size were unchanged across all treatments. Compared to controls, immunohistochemical staining for macrophage makers revealed greater numbers of F4/80+ macrophages in the labyrinth (+36%) of placentas from the 50 ppm groups and junctional zones (+145%, +184%) of the 5 and 50 ppm CdCl<sub>2</sub> treatment groups respectively. Macrophages staining positive for the phagocytosis marker Iba1 were reduced in the placental labyrinth of both 5 ppm (-14%) and 50 ppm (-29%) treatment groups.

**Conclusions:** Exposure to 5 and 50 ppm CdCl<sub>2</sub> during gestation resulted in serum concentrations of Cd similar to pregnant humans and altered the enrichment of placental macrophage subpopulations in the absence of overt fetoplacental toxicity.

**Impact:** This work explores novel mechanisms of cadmium toxicity in the placenta and emphasizes the importance of the innate immune system to placental health.

**P13 1-Trichloromethyl-1,2,3,4-tetrahydro-beta-carboline (TaClo)-Induced Developmental Toxicity and Neurotoxicity in the Zebrafish Model Following the Early-Life Exposure**

*Ji-Hang Yin, Katharine Horzmann*  
Auburn University, Auburn, AL, USA.

**Abstract**

**Introduction:** 1-Trichloromethyl-1,2,3,4-tetrahydro-beta-carboline (TaClo) is an endogenous neurotoxicant formed in the brain after exposure to trichloroethylene (TCE) and tetrachloroethylene (PERC). TCE and PERC are industrial solvents and have the potential to induce developmental toxicity and neurotoxicity; however, it is unknown if their metabolite, TaClo, triggers similar effects in developmental and neural systems. This study tested the hypothesis that embryonic zebrafish exposure to environmentally relevant concentrations of TaClo induces developmental toxicity and neurotoxicity. **Experimental design:** Fertilized embryos were dosed with embryo water (control), DMSO (carrier control, TaClo at 5 ppb, 50 ppb, and 500 ppb, and MPTP (positive control) for 24 or 120 hours post fertilization (hpf). Endpoints for developmental toxicity evaluation include survival and hatching percentage, body measurement, and heart rate measurement. Photomotor and visual motor behavioral response tests, and assessment of relative dopaminergic neuronal numbers in the ventral diencephalon using whole mount in-situ hybridization and immunofluorescence assay were used to assess neurotoxicity. **Results:** TaClo exposed zebrafish showed altered neurobehavior (5 ppb and 500 ppb) at 24 hpf, decreased distance moved and velocity (5 ppb) at 120 hpf, decreased pericardial area (50 ppb) at 120 hpf, and decreased relative dopaminergic neuronal cell numbers in the ventral diencephalon (5 ppb) compared to the carrier. **Conclusion:** Environmentally relevant concentrations of TaClo induced developmental toxicity and neurotoxicity in the zebrafish model following the early-life exposure. **Impact statement:** These results highlight the importance of studying TCE and PERC metabolites and demonstrate TaClo as a developmental and neurotoxicant in the zebrafish model.

**P14 Effects of Soy Isoflavones on Hormone Secretion in the Male Gonad**

*Kristen G. Hoehler, Benson T. Akingbemi*  
Auburn University College of Veterinary Medicine,  
Auburn, AL, USA.

**Abstract**

The two predominant isoflavones in soybeans are genistein and daidzein. Previous reports demonstrated that genistein and daidzein are estrogen-mimicking compounds, which may interfere with male reproductive tract development by disrupting steroid hormone production and function in the male gonad. However, the specific sites of this interference in the male endocrine system have yet to be determined. To identify the proteins affected by soy isoflavones, 21-day-old Long-Evans male rats were fed either a control casein diet, control casein diet plus 300 ppm genistein and 200 ppm daidzein (G+D), or control casein diet plus 600 ppm genistein and 400 ppm daidzein (2G+2D) for 28 days. Serum T concentrations were decreased in the G+D diet group ( $p < 0.05$ ) in association with decreased basal testicular ( $p < 0.05$ ) and basal and LH-stimulated Leydig cell T secretion ( $p < 0.05$ ). However, serum ( $p < 0.05$ ), basal testicular ( $p < 0.001$ ), LH-stimulated testicular ( $p < 0.05$ ) and basal Leydig cell T production ( $p < 0.05$ ) was increased after feeding of the 2G+2D diet. The results of Western blot analyses showed increased estrogen receptor- $\alpha$  expression in the 2G+2D diet group ( $p < 0.05$ ), decreased Cathepsin D expression in the G+D diet group ( $p < 0.001$ ) and the 2G+2D group ( $p < 0.0001$ ), but increased Sirtuin 1 expression in the G+D group ( $p < 0.0001$ ) and 2G+2D group ( $p < 0.00001$ ). These observations imply that soy isoflavones target steroidogenesis possibly through estrogenic mechanisms active in the male gonad and may exert an adverse impact on reproductive development and function. These findings also indicate that phytoestrogens in food products warrant further research in the field of nutritional toxicology.

## P15 Characterization of 3D Models of Human Uterine Endometrium for Use in Evaluating the Role of Environmental Toxicants in Endometrial Cancer

Jingli Liu, Linda Yu, Lysandra Castro, Yitang Yan, Darlene Dixon  
National Institute of Environmental Health Sciences (NIEHS),  
Durham, NC, USA.

### Abstract

Endometrial cancer is the most common gynecological cancer in the US. Currently, there are few suitable *in vitro* cell lines/models that mimic the human endometrium to evaluate the effects of environmental exposures. We developed 3D models of the endometrium to assess the endocrine disrupting effects of chemicals like tetrabromobisphenol A (TBBPA), a ubiquitous flame retardant, that has been shown to induce endometrial cancer in rats in an NTP 2-year assay. We first developed a single-cell type 3D model using human immortalized endometrial epithelial cells (EEC). EEC spheroids treated with TBBPA at 10<sup>-3</sup> mM showed increased cell proliferation, and a receptor tyrosine kinase (RTK) array revealed increased activation of several growth factor receptors, including EGFR, ErbB2, FGFR, Insulin R/IGF-1R and PDGFR that are biomarkers of endometrial cancer. To better mimic the *in vivo* microenvironment, we further explored a 3D multicellular model by coculturing EEC with endometrial stromal cells (ESC), the two major cell types of the endometrium *in vivo*. Optimization of the EEC:ESC at 2:3 ratio was determined by live/dead-cell and cell proliferation assays. Immunofluorescence staining for vimentin and E-cadherin showed spheroid structures with EEC at the periphery and ESC at the inner core, which mimicked the spatial orientation of the endometrium observed *in vivo*. Hormone-responsive studies showed the EEC:ESC spheroids were more sensitive than EEC spheroids to steroid hormones representing the menstrual cycle phases. This study provides 3D models recapitulating endometrial biology that are appropriate for studying the effects and molecular mechanism(s) of environmental toxicants that target the endometrium.

## P16 Intrahepatic Cholangiocarcinoma with Pulmonary Metastasis in a Rhesus Macaque (*Macaca mulatta*)

Andressa Varella Gonsioroski<sup>1</sup>, Mayra Tsoi<sup>1</sup>, Meredith Leigh Cronin<sup>2</sup>, Nicholas Vetter<sup>3</sup>  
<sup>1</sup>Michigan State University, Lansing, MI, USA. <sup>2</sup>Inotiv, Inc, Alice, TX, USA. <sup>3</sup>Inotiv, Inc, Kalamazoo, MI, USA.

### Abstract

Here we describe a unique case of a spontaneous cholangiocarcinoma in a 28-years-old, female Rhesus macaque (*Macaca mulatta*). Rhesus macaques exhibit increased tumor incidence with age as observed in humans. This resemblance makes them a valuable comparative oncology model, emphasizing the need for a comprehensive understanding of spontaneous neoplasia in this species. This animal presented with progressive lethargy and inappetence despite multimodal treatments. Necropsy revealed numerous firm, variably sized, irregular nodules on the liver and lung parenchyma. Histologically, the hepatic parenchyma was markedly replaced and effaced by a highly cellular, poorly demarcated, infiltrative proliferation of neoplastic epithelial cells supported by a scirrhous stroma. Neoplastic cells were arranged in tortuous and dilated tubules lined by a single layer of tall cuboidal to columnar epithelial cells. The neoplasm was bordered by a rim of lymphocytes that blended with non-neoplastic hepatic parenchyma. Similar neoplastic cell population also formed multiple, distinct nodules in the lungs. Neoplastic cells in the liver and lung showed positive immunolabeling for CK7 and negative immunolabeling for Hep-Par1. Histologic and immunohistochemistry findings were consistent with cholangiocarcinoma, which are rare neoplasms in non-human primates, and, to our knowledge, it has not been previously reported as a spontaneous finding in Rhesus macaques.

## P17 MRI and Histological Measures of Myelination Are Correlated in a Rat Model of BPA Neurotoxicity

Bradley C. Wright<sup>1</sup>, Joel P. Levoy<sup>2</sup>, Elizabeth M. Fugate<sup>2</sup>, Diana M. Lindquist<sup>2</sup>, Alex Edmondson<sup>2,1</sup>

<sup>1</sup>University of Cincinnati College of Medicine Department of Environmental and Public Health Sciences, Cincinnati, OH, USA.

<sup>2</sup>Cincinnati Children's Hospital Medical Center Imaging Research Center, Cincinnati, OH, USA.

### Abstract

Bisphenol A (BPA) is ubiquitous in the environment and has previously been shown to alter oligodendrocyte phenotypes, which may dysregulate myelination. Magnetic resonance imaging (MRI) is used to quantify myelination *in vivo*; however, histology is the standard for assessing myelination *ex vivo*. Thus, we seek to validate MRI measures of myelination using histology in a BPA model of neurotoxicity. For this study, 24 Sprague Dawley rats were dosed with BPA (2.5, 25, 250 ug/kg-bw, oral gavage) from birth for 90 days and then imaged on a Bruker 7T MRI scanner where we collected images representing myelination including myelin water fraction (MWF), fractional anisotropy (FA), radial diffusivity (RD), and axial diffusivity (AD). After scans and euthanasia, brains were cryosectioned to 10um and stained with fluoromyelin (myelin), phalloidin (f-actin), and DAPI (nuclei). Histological sections were imaged using epifluorescence microscopy at 4x magnification. Mean MRI intensity and mean luminescence were measured using ImageJ in the corpus callosum, hippocampus, hypothalamus, and cingulate tract. Fluoromyelin was positively correlated (Pearson's Correlation) with MWF ( $r = 0.63$ ,  $p = 4.38e-5$ ), and FA ( $r = 0.60$ ,  $p = 5.39e-11$ ), while being negatively correlated with RD ( $r = -0.43$ ,  $p = 1.35e-5$ ). AD was not positively correlated with fluoromyelin or phalloidin. These results demonstrate that MRI measures represent histological measures of myelination. At this time, no dose effects have been identified in the relationship between histology and MRI. Moving forward we hope to better elucidate dose effects and influence of sex on BPA neurotoxicity.

## P18 Neuropathology Evaluation of Olney Lesions in Regulatory Drug Development Toxicology Studies

Deepa B. Rao<sup>1</sup>, William H. Jordan<sup>2</sup>, David G. Hall<sup>2</sup>

<sup>1</sup>Greenfield Pathology Services, Inc, Ellicott City, MD, USA.

<sup>2</sup>Greenfield Pathology Services, Inc, Greenfield, IN, USA.

### Abstract

Acute neuropathology findings were first described by John Olney et al (1989) following administration of N-methyl-D-aspartate (NMDA) receptor antagonists (such as phencyclidine, MK-801 and ketamine) in adult rats, although findings in other species have since been reported. Initial descriptions of the lesion included neuronal vacuolation (in the posterior cingulate / retrosplenial cortex) with subsequent characterization to include neuronal cell death and/or gliosis. Given the potential of NMDA receptor antagonists to induce Olney lesions, the Food and Drug Administration often requires that sponsors submit, as a part of their Investigational New Drug (IND) submission, additional nonclinical safety data (at least, for the NMDA receptor antagonist class of therapeutic drug candidates). Such nonclinical safety data rests primarily on conducting a specialized "Olney lesion" neurotoxicity study in rats where risk assessment rests on pathomorphological findings. The focus of this presentation is on factors impacting morphological evaluation in Olney lesion studies such as brain-trimming, fixation, embedding, staining, sectioning, and microscopic evaluation techniques. Evaluation of Hematoxylin & Eosin-stained sections under epifluorescent illumination are specifically highlighted as a resource-effective approach to evaluate neuronal cell death in Olney lesion neurotoxicity evaluations. Experimental parameters in the context of study design (such as time-points and inclusion of positive control), as well as interpretation of morphological findings for risk assessment are included.

## P19 Spontaneous Splenic Hemangiosarcoma in a Young Sprague-Dawley Rat

Fei Zhou<sup>1</sup>, Xixing Zhao<sup>2</sup>, Yu Ma<sup>2</sup>, Tiansheng Zhou<sup>2</sup>, Yuanyuan Duan<sup>1</sup>, Hegen Dai<sup>1</sup>, Xihua Wang<sup>1</sup>, Yinghong Hu<sup>1</sup>

<sup>1</sup>Laboratory Testing Division, WuXi AppTec (Chengdu) Co., Ltd. Safety Evaluation Center, Chengdu, Sichuan, China. <sup>2</sup>Laboratory Testing Division, WuXi AppTec (Suzhou) Co., Ltd, Suzhou, Jiangsu, China.

### Abstract

**Objectives:** To report a rare case of spontaneous hemangiosarcoma in a young Sprague-Dawley (SD) rat.

**Material & Method:** This 9-week-old male SD rat was assigned to the mid-dose group in a 14-day non-GLP toxicity study. Gross observation was conducted and a full panel of tissues was microscopically evaluated after hematoxylin and eosin staining. In addition, Immunohistochemistry (IHC) staining was conducted with a CD 31 marker.

**Results:** Macroscopically, the spleen was not observed in the abdominal cavity, rather, a multinodular mass was noted at the location of the spleen. Microscopically, 90% the spleen was effaced by an unencapsulated, poorly demarcated, densely cellular neoplasia, adjacent large necrotic area, and marked hemorrhage. The neoplastic cells had indistinct cell borders, a small amount of eosinophilic fibrillar cytoplasm, and a variably sized, oval to elongate nucleus with coarse chromatin and one or multiple distinct basophilic nucleoli. Mitoses average 3-4 per HPF. CD31 IHC staining showed strong cytoplasmic positive in the neoplastic cells, suggesting an endothelial cell origin.

**Conclusion:** Hemangiosarcoma is common in aged rodents but rare in young rats. In this case, based on the microscopic characteristics and the positive CD31 staining, we consider this tumor to be a hemangiosarcoma. Though this change occurred in the treatment group, but only occurred in one mid-dose animal and none in the low-dose and high-dose groups, and a short-term study indicated that this neoplasia was spontaneous.

**Impact statement:** Spontaneous hemangiosarcoma in the young SD rats will enrich the background data on the neoplasm in the young laboratory animals.

**P20 Poster Withdrawn**

## P21 Anticoagulant Rodenticide Toxicity in Three Red-Tailed Hawks (*Buteo jamaicensis*) from Northeastern Massachusetts

Jiashi Feng<sup>1</sup>, Julia Lombardo<sup>1,2</sup>, Felix Valles Feliciano<sup>1,2</sup>, Erin Hutchings<sup>3</sup>, Brittany Rasche<sup>1,2</sup>

<sup>1</sup>Department of Diagnostic Medicine/Pathobiology, College of Veterinary Medicine, Kansas State University, Manhattan, Kansas, USA. <sup>2</sup>Kansas State Veterinary Diagnostic Laboratory, Manhattan, Kansas, USA. <sup>3</sup>Cape Ann Wildlife, Inc, Essex, Massachusetts, USA.

### Abstract

**Introduction:** Anticoagulant rodenticide (AR) toxicity in raptors, such as bald eagles and red-tailed hawks, has been reported across North America as an unintentional consequence of chemical rodent control. Multiple wild red-tailed hawks (*Buteo jamaicensis*) have presented to Cape Ann Wildlife, Inc. in northeastern Massachusetts for acute weakness and bloody fluid exuding from the mouth, suspicious of AR toxicity. **Methods and Materials:** Three deceased red-tailed hawks were submitted to the Kansas State Veterinary Diagnostic Laboratory for necropsy and collection of fresh liver for toxicological analysis. For two birds, representative tissue samples were fixed in 10% neutral buffered formalin and routinely processed with hematoxylin and eosin stains. **Results:** All hawks displayed hemorrhage of varying severity in the lungs, air sacs, and coelomic cavity with no gross evidence of trauma. Histologic examination confirmed acute pulmonary hemorrhage without associated inflammation or vasculitis. Toxicological analysis of fresh liver samples for anticoagulant rodenticides revealed the presence of brodifacoum (26.13-341.33 parts per billion) and difethialone (150.30-235.71 parts per billion) in all three birds. **Conclusion:** Significant pulmonary and/or cavitory hemorrhage likely resulted in the death of these three red-tailed hawks. Given the absence of other causes of hemorrhage (trauma, hepatic failure, etc.) and detection of anticoagulant rodenticides within the liver, AR toxicity was considered the most likely cause of death. **Impact statement:** The use of second-generation AR, including brodifacoum and difethialone, poses a significant risk to non-target wildlife species such as red-tailed hawks. AR toxicity should be considered in raptors presenting with acute weakness and hemorrhage.

**P22 Exploring the Potential of Natural Compound 6'-Hydroxy Justicidin B as a Therapeutic Agent against COVID-19: *In Vitro* and *In Vivo* Nonclinical Efficacy and Toxicity Studies following Good Laboratory Practice Standards**

Byoung-Seok Lee<sup>1</sup>, Min Heui Yoo<sup>1</sup>, Han Young Eom<sup>1</sup>, Kang-Hyun Han<sup>1</sup>, Joung-Wook Seo<sup>1</sup>, Junguk Choi<sup>2</sup>, Jihyun Jeon<sup>2</sup>, Sangho Lee<sup>2,3</sup>, Seungtaek Kim<sup>4</sup>, Yong-Bum Kim<sup>1</sup>

<sup>1</sup>Department of Advanced Toxicology Research, Korea Institute of Toxicology, Daejeon, Republic of Korea. <sup>2</sup>Research Institute, Dong-Wha Pharmaceutical Company, Yongin, Republic of Korea. <sup>3</sup>School of Pharmacy, Sungkyunkwan University, Suwon, Republic of Korea. <sup>4</sup>Zoonotic Virus Laboratory, Institute Pasteur Korea, Seongnam, Republic of Korea.

**Abstract**

**Background:** Since the onset of the coronavirus disease 2019 (COVID-19) pandemic, remarkable advances have been made in vaccine development to reduce mortality. Despite this, therapeutic treatments for COVID-19 are comparatively limited. The study's goal is to assess the effectiveness and safety of 6'-hydroxy justicidin B (6'-HJB), a compound from *Justicia procumbens* known in traditional Chinese medicine for its antiviral properties, against SARS-CoV-2, in order to determine its potential as a COVID-19 treatment. **Study Design:** The research involved synthesizing the primary component of *J. procumbens*, 6'-HJB, followed by conducting antiviral efficacy studies and nonclinical toxicology research. **Methods:** To evaluate the efficacy and safety of 6'-HJB, both *in vitro* and *in vivo* methodologies were utilized. The safety assessment included toxicokinetics, safety pharmacology, and GLP toxicity evaluations, including single-dose and repeated-dose toxicity studies in dogs. **Results:** Assays adhering to nonclinical Good Laboratory Practice (GLP) standards using Calu-3 cell line revealed that 6'-HJB demonstrates superior efficacy against SARS-CoV-2 and lower toxicity than existing antiviral drugs. Single-dose and four-week repeated oral toxicity studies in Beagle dogs established minimal harmful effects at considerable dosages. The lethal dose of 6'-HJB exceeded 2,000 mg/kg in Beagle dogs; therefore, we established a no-observed-adverse-effect level of 1,000 mg/kg in Beagle dogs, suggesting a substantial safety margin. Toxicokinetic and GLP safety pharmacology studies demonstrated no adverse effects on metabolic processes, respiratory or central nervous systems, or cardiac function. **Conclusion:** These comprehensive analyses suggest that 6'-HJB has significant potential as a novel antiviral therapeutic agent for COVID-19 treatment.

**P23 Assessment of 6'-Hydroxy Justicidin B as a Potential Therapeutic for COVID-19: Nonclinical Efficacy and Good Laboratory Practice (GLP) Toxicity Studies *In Vitro* and *In Vivo***

Ji-Seok Han<sup>1</sup>, Min Heui Yoo<sup>1</sup>, Tae-Yang Jung<sup>1</sup>, Heejin Park<sup>1</sup>, Eun Mee Lee<sup>1</sup>, Min Seng Jang<sup>1</sup>, Seng-Min Back<sup>1</sup>, Yunha Hwang<sup>2</sup>, Jihyun Youm<sup>2,3</sup>, Yong-Bum Kim<sup>1</sup>

<sup>1</sup>Department of Advanced Toxicology Research, Korea Institute of Toxicology, Daejeon, Republic of Korea. <sup>2</sup>Research Institute, Dong-Wha Pharmaceutical Company, Yongin, Republic of Korea. <sup>3</sup>Graduate School of East-West Medical Science, Kyung Hee University, Yongin, Republic of Korea.

**Abstract**

**Introduction:** Over six years have passed since the onset of the coronavirus disease 2019 (COVID-19) pandemic. Significant advancements in vaccine development have been made, effectively reducing the prevalence and mortality of the disease. This study aims to investigate the efficacy and safety of 6'-HJB against COVID-19, focusing on its potential as a promising therapeutic agent. **Experimental Design:** The research involved the synthesis of 6'-HJB and conducting extensive antiviral efficacy tests against SARS-CoV-2, as well as non-clinical Good Laboratory Practice (GLP) studies. **Methods:** To assess the effectiveness of 6'-HJB against COVID-19, *in vitro* experiments were conducted using African green monkey kidney epithelial (Vero) cells. Additionally, non-clinical GLP toxicity studies, including genotoxicity and both single and repeated dose toxicity studies using rodents, were carried out. **Results:** Genotoxicity tests revealed no genotoxic effects of 6'-HJB. In the toxicity studies, single and 4-week repeated oral administrations were performed on Sprague Dawley rats. These studies demonstrated that the lethal dose of 6'-HJB exceeded 2000 mg/kg, and the no-observed-adverse-effect level (NOAEL) for repeated dosing was also established at 2000 mg/kg in rats, affirming its safety. **Conclusion:** The efficacy of 6'-HJB against COVID-19 and the results of the non-clinical GLP toxicity tests highlight the potential of 6'-HJB as a novel therapeutic intervention for COVID-19 treatment. **Impact Statement:** This research contributes to the expanding arsenal of medical strategies against COVID-19 and could play a crucial role in reducing the burden of the pandemic on healthcare systems and societies worldwide.

## P24 Pyogranulomatous Inflammation Associated with an Extended-Release Buprenorphine Injection Formulation in Rabbits

*Lori E. Bedient, Eleana R. Sosnowski, L. Michele Wilkinson*  
Labcorp Early Development Laboratories, Somerset, NJ, USA.

### Abstract

Compounded formulations of Buprenorphine HCl Extended-Release Polymer Injection solution (BUP-ER) offer convenient, long-acting pain control for laboratory animals. Several long-acting buprenorphine formulations have recently been reported to cause significant injection site reactions in non-human primates and rodents. Similar injection site reactions to BUP-ER have been observed at our facility in Gottingen minipigs after telemetry device implantation. To study the development of these injection site reactions, BUP-ER in either 1 mg/ml (dose volume 0.1 ml/kg) or 3 mg/ml (dose volume 0.03 ml/kg) concentrations or USP grade Buprenorphine HCl solution (BUP) 0.3 mg/ml (dose volume 0.17 ml/kg) as a control were subcutaneously injected into the interscapular tissue of rabbits. Animals were euthanized over the course of 4 weeks at 1-week intervals for histologic assessment of the injection sites, major organs and draining lymph nodes. At necropsy, discolored masses at the injection sites were observed macroscopically in four of six animals administered 1 mg/ml BUP-ER and five of six animals administered 3 mg/ml BUP-ER. Severe, locally extensive pyogranulomatous inflammation was noted in the subcutis in animals that received BUP-ER 1 mg/ml and 3 mg/ml concentrations. No associated findings were identified in the remaining examined tissues. No macroscopic or microscopic findings of injection site reactions were noted in control animals administered BUP. These results demonstrated localized pyogranulomatous inflammation in rabbits up to 4 weeks after subcutaneous administration of BUP-ER consistent with reports in other species.

## P25 Presumptive Red Maple Leaf Toxicosis in a Horse

*Luan C. Henker<sup>1</sup>, Danyue Kang<sup>2</sup>, Thainá Lunardon<sup>1</sup>, Rachel Neto<sup>1</sup>*  
<sup>1</sup>Auburn University, Auburn, Alabama, USA. <sup>2</sup>The Ohio State University, Columbus, Ohio, USA.

### Abstract

**Introduction:** Red maple (*Acer rubrum*) is native to the eastern United States. This plant has been associated with sporadic intoxication in horses that commonly occurs during the summer and fall seasons. Ingestion of dried or wet/wilted red maple leaves may cause oxidative damage to erythrocytes and hemoglobin, resulting in hemolytic anemia, methemoglobinemia, and formation of Heinz bodies and eccentrocytes. The toxic compound is still unknown. **Case report:** In May 2023, a 16-year-old Quarter Horse gelding was presented to Auburn University for a 3-day history of lethargy, marked anemia, and cyanotic oral mucous membranes. Laboratory findings included a packed cell volume of 15.3% [reference interval (RI): 32.0-48.0], elevated mean corpuscular hemoglobin concentration (MCHC) (61.1 g/dL; RI: 31.0-37.0), and a high hemolysis index (1642; RI: 0-43). Blood smears revealed moderate amounts of ghost cells and eccentrocytes within a highly hemolytic background. The animal died naturally and was submitted for necropsy. The main gross findings included bilateral dark-red discoloration of the kidneys and the urinary bladder contained moderate amounts of dark-red, thin, urine (hemoglobinuria). A moderate number of cortical tubules were variably dilated, lined by attenuated epithelial cells, and filled with hemoglobin casts. Multifocally, tubular epithelial cells contained a small amount of brown cytoplasmic pigment that was highlighted with Prussian blue (consistent with iron). **Conclusion:** The diagnosis of presumptive maple leaf toxicity was made based on the gross and histologic findings, and the absence of other potential causes of hemolytic anemia.

## P26 Histologic Assessment of Inflammation in Mouse Models of Inflammatory Bowel Disease Using Digital Pathology

*Morgan Maisel, Sean Graham, Katie Malley, Caroline Morel, Brendan Oakes, Andrew McKnight, Dinesh Bangari*  
Sanofi, Cambridge, MA, USA.

### Abstract

**Introduction:** Inflammatory bowel disease (IBD) imposes a significant disease burden on patients. The lack of efficacious and long-lasting treatments necessitates the development of animal models for translational research and drug discovery. Detailed histologic characterization of these models is critical for their translatability in drug development. In this study, we integrated manual and digital histopathology approaches to gain qualitative and quantitative pathology insights from three mouse models of IBD. **Methods:** Routine hematoxylin and eosin staining and immunohistochemistry (IHC; CD45, CD68, and Iba1) were performed on formalin-fixed paraffin-embedded sections of colon from an adoptive transfer naïve T-cell (TCT) induced-colitis model, a CD40 agonist monoclonal antibody-induced colitis model, and a 2,4,6-trinitrobenzene sulfonic acid (TNBS)-induced colitis models of IBD. Semi-quantitative scoring assessing the number of infiltrating inflammatory cells was performed by a board-certified pathologist and was then compared to data generated via digital analysis of IHC images quantifying the number of inflammatory cell infiltrates. **Results:** Disease induction was confirmed with histopathology in each model. Quantitative data from the image analysis software correlated with the semi-quantitative data from the pathologist scoring in all but the CD68+ cell population in the TNBS model when compared to control animals. **Conclusion:** Quantitative data can provide more precise information in the histologic characterization of mouse models of IBD. **Impact Statement:** Image analysis can provide quantitative information on the phenotype of animal disease models, can be included as part of the histologic characterization of new models, and can be used to inform future applications.

## P27 Assessment and Validation of Deep Learning Algorithms in Identifying Early Chronic Progressive Nephropathy Changes

*Priyanka Thakur<sup>1,2</sup>, David Cunefare<sup>1,2</sup>, Charan Ganta<sup>1,3</sup>, Cynthia Willson<sup>1,3</sup>, Allison C. Boone<sup>1,4</sup>, Katherine Allen-Moyer<sup>5</sup>, Keith Shockley<sup>6</sup>, Eli Ney<sup>1</sup>, Ronald Herbert<sup>1</sup>, Mark Cesta<sup>1</sup>*

<sup>1</sup>Division of Translational Toxicology, National Institute of Environmental Health Sciences, Research Triangle Park, NC, USA.

<sup>2</sup>Charles River Laboratories, Durham, NC, USA. <sup>3</sup>Inotiv, Morrisville, NC, USA. <sup>4</sup>Experimental Pathology Laboratories, Inc., Morrisville, NC, USA. <sup>5</sup>Social and Scientific Systems, Inc., a DLH Holdings Corp Company, Durham, NC, USA. <sup>6</sup>Division of Intramural Research, National Institute of Environmental Health Sciences, Research Triangle Park, NC, USA.

<sup>1</sup>Division of Translational Toxicology, National Institute of Environmental Health Sciences, Research Triangle Park, NC, USA.

### Abstract

**Introduction:** Convolutional neural networks (CNNs) based deep learning (DL) methods of artificial intelligence (AI) have rarely been used for lesion identification in diagnostic histopathology and have the potential to identify early changes of chronic progressive nephropathy (CPN) in rodent studies. **Methods and Materials:** Hematoxylin and eosin (H&E) stained kidney tissue sections from two sub-chronic rodent Division of Translational Toxicology (DTT; formerly, NTP) studies were retrospectively evaluated for early CPN changes using AI. **Experimental Design:** The initial CPN AI algorithm (APP1) was trained on regions of interest (ROIs) extracted from 23 whole slide images (WSIs) from a single study (Study 1). In a second AI algorithm (APP2), we modified our original algorithm by integrating extra training slides from another study (study 2). Two board-certified veterinary pathologists annotated validation data sets using the diagnostic criteria established for training. Dice coefficient, sensitivity, and precision metrics were calculated to assess the agreement between the AI and pathologist annotations. **Results:** Compared to APP1, APP2 increases precision. However, other metrics (dice coefficient and sensitivity) were equivalent between APP1 and APP2. Both algorithms detected a greater number of CPN lesions than the pathologists. **Conclusion:** Compared to APP1, APP2 reduced the over-detection of not true CPN lesions in study 2, which indicates that five additional training slides from the study can impact the algorithm's rate of over-detection within that study. **Impact Statement:** These algorithms could increase the sensitivity for detecting early CPN and reduce the time spent by pathologists in identifying subtle early CPN lesions to provide quick decision support.

## P28 Early Deaths of Rabbits Resulting from Potential Pregnancy Toxemia in a Developmental Toxicity Study

Rongrong Li, Tiansheng Zhou, Rong Xu, Lin Zhu, Lei Wang, Xixing Zhao  
WuXi AppTec (Suzhou) Co., Ltd., Suzhou, Jiangsu, China.

### Abstract

**Introduction:** Pregnancy toxemia is a life-threatening metabolic disorder typically seen in late rabbit pregnancies. This study described the clinical symptoms and macroscopic and microscopic findings in control pregnant rabbits that succumbed to this disorder. **Study Design:** Twenty-six 6-month-old pregnant *New Zealand White* rabbits were used as controls in an embryo-fetal developmental toxicity study. They were given a control article, Kollidon VA64 and TPGS 1000, by oral administration once daily from gestation day (GD) 6 to GD 19. Eight early deaths were reported between GDs 18 to 26. **Methods:** Clinical signs, animal body weights, and food consumption were regularly monitored. Gross and histopathological evaluations were conducted on all early deaths. **Results:** All early deaths showed sudden declines in appetite and/or weight loss (up to 10%). These were likely attributed to compression on the gastrointestinal tract by the fetus, leading to decreased intestinal transit and digestion disruption. Key microscopic findings included hepatocellular steatosis (correlated macroscopically with pale discoloration) and hepatocellular necrosis in variable severity, which were likely caused by glucose depletion and fat mobilization due to the high nutritional demands in the late-stage of fetal development and accumulation of ketone bodies during fat mobilization, respectively. These histopathological changes are consistent with characteristics of pregnancy toxemia in rabbits. **Conclusions:** All early deaths were attributed to pregnancy toxemia occurring in late pregnancy. **Impact Statement:** Revealing pregnancy toxemia in this rabbit developmental toxicity study could facilitate interpreting preclinical study data and implementing timely interventions to mitigate its effects in such studies.

## P29 Common Spontaneous Neoplastic Findings in Tg.rasH2 Mice Used in Nonclinical Research Studies

Victoria A. Laast, Alok K. Sharma  
Labcorp Early Development Services Inc, Madison, Wisconsin, USA.

### Abstract

**Introduction:** Currently, the use of 26-week Tg.rasH2 transgenic mouse models (CByB6F1-Tg(HRAS)2Jic) is generally accepted as a substitute for the standard two-year carcinogenicity mouse bioassay by the regulatory agencies. This retrospective analysis of the spontaneous tumor incidences from 26-week carcinogenicity studies is to serve as a reference source from a robust historical database for the types, incidence, and range of background neoplastic findings in these types of studies. Comparison to the available published literature was also made to determine possible genetic shift over the years.

**Methods:** A retrospective evaluation of historical control data was performed on the recorded neoplastic findings in control Tg.rasH2 mice from 26-week carcinogenicity studies completed between 2014 and 2023 at Labcorp Early Development Services Inc. Madison-US site. These data consisting of 47 male and 46 female studies were tabulated for the spontaneous neoplastic findings.

**Results:** Bronchiolo-alveolar adenoma and hemangiosarcoma in the spleen were the most commonly occurring neoplasm (6.3% and 3.8%, males vs 2.3% and 3.5%, females) with hemangioma and hemangiosarcoma being the most frequent neoplasm recorded in other tissues/organs other than the spleen. Neoplastic findings with rare occurrence (less than 1%), included Harderian gland adenoma or carcinoma, malignant lymphoma, squamous cell carcinoma, malignant mesothelioma, and benign/malignant thymoma.

**Conclusion:** Although the incidences varied slightly when compared with previously reported literature, the types of tumors did not vary significantly, confirming robustness of this animal model.

**Impact statement:** Presented information will be beneficial to pathologists to discern spontaneous versus test article-related effects in Tg.rasH2 mice.

## P30 Whole Brain Assessment of Myelin in a Rat Model of Bisphenol-A Exposure

Alex Edmondson<sup>1,2</sup>, Bradley Wright<sup>2,1</sup>, Joel Levoy<sup>1</sup>, Beth Fugate<sup>1</sup>, Diana Lindquist<sup>1,2</sup>

<sup>1</sup>Cincinnati Children's Hospital Medical Center, Cincinnati, OH, USA. <sup>2</sup>University of Cincinnati College of Medicine, Cincinnati, OH, USA.

### Abstract

Years of epidemiological research have associated anxious behavior in children to exposure to the endocrine disrupting chemical (EDC), Bisphenol-A (BPA). However, other EDCs have also been implicated, thus confounding the role of EDCs on mental health. Because BPA has been associated with influencing oligodendrocyte differentiation and maturation, we have developed a translational neuroimaging rat model to investigate the role BPA plays on myelination and anxiety. 24 Sprague Dawley rats were used in this study. Beginning at P1, rats were dosed with BPA (2.5, 25, 250 µg/kg-bw, oral gavage). 2D high-resolution T2-weighted images and Diffusion Tensor Imaging (DTI) were acquired on rats on a Bruker 7T MRI scanner *in vivo* prior to euthanasia at P60 and P90. Using software we developed to co-register T2w and DTI images to an anatomical atlas (SIGMA), we extracted predefined regions of interest (ROI) and created ROI x ROI correlation matrices representative of whole-brain myelination relationships in each Dose x Timepoint group. Euclidean distance (ED) was calculated to assess similarity between each matrix. We found that matrices representing different measures of diffusion within Low and High dose at P60 and P90 were more similar within P60 (ED mean = 24.56) than within P90 (ED mean = 86.15), thus suggesting a potential differential time effect on whole brain myelination, possibly due to BPA exposure. However, it is premature to conclude much beyond this. This is a work-in-progress; however, this method of analysis will be an essential for translating our neuroimaging rat model results to human studies.

## P31 Performance Evaluation of Standard vs. Automated AI-Based Image Analysis of Hepatic Necrosis in KO vs. WT mice Infected with *Listeria Monocytogenes*

Charan Ganta<sup>1,2</sup>, David Cunefare<sup>1,3</sup>, Priyanka Thakur<sup>1,3</sup>, Prashant Rai<sup>1</sup>, Eli Ney<sup>1</sup>, Michael Fessler<sup>1</sup>, Ronald Herbert<sup>1</sup>

<sup>1</sup>National Institute of Environmental Health Sciences, Durham, NC, USA. <sup>2</sup>Inotiv, Morrisville, NC, USA. <sup>3</sup>Charles River Laboratories, Durham, NC, USA.

### Abstract

**Introduction:** Semiquantitative scoring of microscopic lesions is a gold standard practice in experimental/toxicologic pathology, however it is affected by intra- and inter-observer variability. With the emergence of artificial intelligence (AI) based image analysis, routine and time intensive evaluation could be automated and applied to repeat experimental studies. Here, we evaluated the performance of AI-based quantitative analysis with standard histopathological evaluation of *Listeria* induced hepatic necrosis/inflammation. **Experimental design:** Of the 16 whole slide liver images, 8 were used for training and the remaining 8 for validation using an AI-based image analysis software. **Methods:** Two AI algorithms were trained, the first for tissue detection using a U-net convolutional neural network (CNN) at 4X resolution followed by a second using a DeepLab CNN at 20X magnification to detect necrosis/inflammation. The segmentations from these algorithms were used to determine the total tissue area and area of necrosis/inflammation for each image. The AI algorithms were validated against the diagnoses of two expert pathologists over 24 equally sized Regions of Interest (ROIs) evenly spread across the 8 validation images. **Results:** Compared to AI, the pathologist who was not involved in training had an average Dice's coefficient of .82; and the two pathologists compared to one another had an average Dice's coefficient of .84 across all images. **Conclusion:** There was a high correlation between the AI and standard histopathological evaluation for detecting liver necrosis/inflammation. **Impact statement:** This suggests, AI algorithm application can be applied to future studies with hepatic necrosis/inflammation.

## P32 Enabling Rat Bone Marrow Cell Lineage Identification in H&E Whole Slide Images Using Multiple IHC-Guided Deep Learning Models

*Edgar A. Rios Piedra<sup>1</sup>, Marco Tecilla<sup>2</sup>, Ines Berenguer Veiga<sup>2</sup>, Kerstin Hahn<sup>2</sup>, Pierre Maliver<sup>2</sup>, Jeff Eastham<sup>3</sup>, Adeyemi O. Adedeji<sup>3</sup>, Shari Lau<sup>3</sup>, Miriam Baca<sup>3</sup>, Ruth Sullivan<sup>3</sup>*

<sup>1</sup>Genentech Inc, South San Francisco, CA, USA. <sup>2</sup>Hoffmann - La Roche Ltd., Basel, Basel-Stadt, Switzerland. <sup>3</sup>Genentech Inc., South San Francisco, CA, USA.

### Abstract

**Introduction:** Hematoxylin and eosin (H&E)-stained bone marrow tissue sections are routinely assessed in toxicologic pathology studies. Although evaluation can be augmented with immunohistochemical (IHC) labeling, IHC is not a standard practice for routine BM assessment. We hypothesized that we could develop computational approaches to predict IHC labeling patterns of cells on H&E-stained BM tissue sections using deep learning (DL) algorithms trained on IHC-informed H&E-based ground truth to enhance routine evaluation of BM cell lineages.

**Methods:** We developed a DL-based segmentation pipeline to predict cellular IHC-expression patterns on H&E slides. Rat formalin-fixed paraffin-embedded decalcified sternum slides were stained and de-stained to generate H&E and IHC from the same section. Whole slide images (WSI) were acquired and aligned (registered) to enable pathologist-generated multimodal ground truth. Then, the IHC-expression model was trained on the H&E slides and IHC labels, developing an independent model for each IHC marker. Results were aggregated and segmentations created for each cell in the marrow section, providing an estimate of IHC expression and other endpoints (e.g., cell density). Endpoints can be made available to enhance results interpretation and communication.

**Results and conclusion:** We successfully developed an AI-enabled method to augment the utility of H&E WSI analysis with predicted IHC marker expression results. This methodology may extend routine BM analysis, trigger additional studies (e.g., BM smears cytology) to further investigate cell population shifts, increase pathologists' confidence when diagnosing BM pathology samples, and provide quantitative data for results visualization and communication.

## P33 The Development and Optimization of a Novel Image Analysis Solution for the Detection of Low-Grade Thyroid Follicular Cell Hypertrophy in Rats

*James Baily<sup>1</sup>, Stuart Naylor<sup>1</sup>, James Alibhai<sup>1</sup>, Elizabeth McInnes<sup>2</sup>*

<sup>1</sup>Charles River Laboratories, Edinburgh, Scotland, United Kingdom. <sup>2</sup>Jealott's Hill International Research Centre, Bracknell, Berkshire, United Kingdom.

### Abstract

**Introduction:** Variability in both the appearance of control thyroids and pathologists' thresholds results in inconsistent diagnosis of low-grade thyroid follicular hypertrophy. Image analysis (IA) solutions have the potential to improve diagnostic certainty in this area.

**Experimental Design:** The established mean epithelial area method of assessing follicular hypertrophy was compared with a novel approach analyzing only intact follicles.

**Methods:** IA models were created in Visiopharm software using 107 training regions from 62 WSIs of rat thyroid. Separate IA models were created to detect individual intact follicles and all follicular and interstitial cells. Algorithms were run on 30 animals per sex from two separate studies with known follicular cell hypertrophy. Two Fixed Calculation Methods and three Empirical Models were developed by comparison against consensus scores generated by 4 pathologists. Empirical Models were applied to 100 control thyroids and compared with each other.

**Results:** The Fixed Calculation Methods - mean epithelial area and epithelial area to colloid area ratio - yielded similar R<sup>2</sup> values. The three Empirical Models, based on mean follicle diameter and epithelial height and on combined outputs of the two fixed calculations - produced markedly improved R<sup>2</sup> scores.

**Conclusion:** Empirical Models using data from the individual follicle detection algorithm were superior to the mean epithelial area fixed calculation approach in the detection of thyroid follicular cell hypertrophy.

**Impact Statement:** The image analysis / data analysis approaches described can be used to support pathologist decision making in cases of equivocal thyroid follicular hypertrophy.

## P34 Unraveling the Complexity of Injection Site Reactions Using Spatial Transcriptomics, Proteomics & Histopathology in an Ex Vivo Human Skin Model

Deidre A. Dalmas<sup>1</sup>, Ali Ebrahimi<sup>1</sup>, Chavon Williams<sup>1</sup>, LiJun Zhou<sup>2</sup>, Kelly Diegel<sup>3</sup>, Thilo Werner<sup>4</sup>, Susan Laffan<sup>4</sup>, H. Christian Eberl<sup>4</sup>, Kate Annunziato<sup>5</sup>

<sup>1</sup>Investigative Safety, *In Vitro In Vivo* Translation (IVIVT), GSK, Collegeville, PA, USA. <sup>2</sup>Non-Clinical Molecular Histology, IVIVT, GSK, Collegeville, PA, USA. <sup>3</sup>Pathology, IVIVT, GSK, Collegeville, PA, USA. <sup>4</sup>Genomics Sciences, GSK, Heidelberg, Germany. <sup>5</sup>Nonclinical Toxicology, ViiV Healthcare, Branford, CT, USA.

### Abstract

Injection site reactions (ISRs) can lead to early termination of compounds in clinical trials, and reduced patient compliance for marketed drugs. Useful preclinical models for the prediction of ISRs are limited. This study explores the use of spatial transcriptomics (ST), proteomics and histopathology for a multi-faceted approach to better understanding of ISRs. Surgically-derived human skin sections were injected with vehicle, or clinically-relevant concentrations of Atenolol (negative control) or positive controls known to induce clinical ISRs [doxorubicin (DOX) or vincristine (VIN)]. Skin was maintained in culture for 4 days and processed to formalin-fixed, paraffin-embedded blocks. ST was conducted/analyzed using FFPE sections, 10X Genomics Visium methodology along with SpaceRanger, Seurat and a novel unsupervised clustering method. Quantitative proteomics was performed using isobaric mass tagging. Ingenuity Pathway Analysis and Gene Ontology enrichment were employed for gene and protein set enrichment, respectively, and association with biological and disease functions. Histopathologic ally, degenerative keratinocyte changes were present in DOX and VIN-treated samples. Thirteen distinct molecular subregions were identified, exhibiting unique spatial gene expression profiles for each treatment. DOX treatment resulted in two spatial clusters with disparate gene expression profiles compared to the controls, which correlated with findings from bulk proteomics data. Similar findings with some differences based on the pathophysiological response were observed for VIN-treated samples vs vehicle control. The study highlights the ability of ST to elucidate spatial gene expression patterns and molecular responses associated with ISRs in ex-vivo human skin. The model may be useful in the understanding of ISRs in the preclinical translational space.

## P35 Single-Cell Finding Detection and Quantification for Cellular-Level Microscopic Findings Using Deep-Learning Approaches

Hope Williams<sup>1</sup>, Jogile Kuklyte<sup>1</sup>, Laoise Lord Bissett<sup>1</sup>, Sarah Marcu<sup>1</sup>, Esther Crouch<sup>2</sup>, Lise Bertrand<sup>2</sup>, Daniel Rudmann<sup>2</sup>, Pierre Moulin<sup>1</sup>

<sup>1</sup>Deciphex, Dublin, Ireland. <sup>2</sup>Charles River Laboratories, Fredrick, MD, USA.

### Abstract

**Introduction/Objectives:** Identification of single-cell findings for example, single-cell necrosis and mitotic-figures, is important in the histologic evaluation of toxicologic pathology studies. The grading and quantification of these findings is time-consuming and subjective, pathologist efficiency may be aided by quantitative analysis. Deep-learning based object detection (OD) models can be trained with single-cell annotations on whole slide images (WSIs) to efficiently detect rare findings on unseen slides in a standardized manner.

**Methods and Materials/Experimental Design:** Pathologists annotated 1,200 examples of necrotic/apoptotic and mitotic cells across 225 WSIs (19 studies). Classifiers were trained and evaluated using predictive masks on annotated and unannotated studies both qualitatively by a pathologist, and quantitatively by the data science team. False positive or false negative detections were correctly annotated to improve classifier detection.

**Results:** The developed classifier is evaluated on three generalization levels: 1) tile, 2) slide, and 3) study. Up to 15% of the annotated data was set aside as a blinded validation set; sensitivity (recall) of the classifier was calculated on this data. Results on unseen study data show generalization capabilities of the solution to scanner, tissue processing, or other variations. Density of the detections is also estimated on full WSI images to qualitatively assess the specificity of the results.

**Conclusion/Impact Statement:** This methodology enables reliable and swift detection of individual mitotic and necrotic/apoptotic cells in rat liver slides, as well as precise computer-assisted quantification. The approach could also be expanded to other species and tissue types with minimal requirement for additional data.

## P36 Development of AI Classifiers and Integration into a Commercially Available Decision Support Tool for Toxicologic Pathology

Jogile Kukyte<sup>1</sup>, Laiose Lord Bissett<sup>1</sup>, Hope Williams<sup>1</sup>, Eoghan Keany<sup>1</sup>, Esther Crouch<sup>2</sup>, Lise Bertrand<sup>2</sup>, Daniel Rudmann<sup>2</sup>, Pierre Moulin<sup>1</sup>

<sup>1</sup>Deciphex, Dublin, Ireland. <sup>2</sup>Charles River Laboratories, Fredrick, MD, USA.

### Abstract

**Introduction:** In drug development, animal studies are crucial for screening compounds and assessing their safety before moving to clinical trials. Pathologists evaluate tissues at the microscopic level to characterise potential targets of toxicity. To assist pathologists in this process, we selected 15 organs and 47 lesions that are commonly encountered in subacute rat studies for AI model development.

**Methods:** We developed pixel segmentation classifiers for all prioritised organs and lesions. Object-based detection classifiers were developed to address single cell findings like mitoses or apoptotic cells. Density-based approaches were applied to lesions including hepatocellular hypertrophy. A ground truth definition and annotation criteria was defined for each lesion, based on internationally accepted terminology.

**Results:** A suite of classifiers, qualitatively and quantitatively qualified by board-certified pathologists and data scientists, were integrated into the digital study review workflow. Pathologists were provided with coloured mask overlay on the tissue image that highlighted the probability that the specific lesion was present.

**Conclusions:** It is our aspiration that sharing our experiences will assist other developers in focusing on key aspects, leading to the development of classifiers that enhance workflow efficiency in classifier training, design and testing, and prioritisation for the toxicologic pathologist. These tools will enhance the pathologists' workflow and efficiency by supporting lesion detection and assessment in nonclinical animal studies.

## P37 13-Week Repeat-Dose Rat Intrathecal Toxicity Studies for Four MOE ASOs Intended for the Treatment of Nano-Rare Neurological Disease

Lisa Berman-Booty<sup>1</sup>, Christine Hoffmaster<sup>1</sup>, Julie Veyssiere<sup>2</sup>, Claudine Tremblay<sup>2</sup>, Erica Twitchell<sup>3</sup>, Nicole Hamelin<sup>2</sup>, Luc Chouinard<sup>2</sup>, Catherine Parisien<sup>4</sup>, Julie Douville<sup>4</sup>, Scott Henry<sup>1</sup>

<sup>1</sup>Ionis Pharmaceuticals, Carlsbad, CA, USA. <sup>2</sup>Charles River Laboratories, Montreal, Quebec, Canada. <sup>3</sup>Charles River Laboratories, Shrewsbury, MA, USA. <sup>4</sup>n-Lorem Foundation, Carlsbad, CA, USA.

### Abstract

Nano-rare diseases are diseases caused by a unique mutation identified in fewer than 30 people worldwide. By modulating target gene expression, antisense oligonucleotides (ASOs) provide a unique therapeutic approach for the treatment of many genetic diseases. The versatility of ASO technology makes it amenable to address nano-rare diseases. Since these diseases are often severe, debilitating, and life-limiting, the FDA has created unique guidelines to support investigative new drug applications for the development of such ASOs. Specifically, the FDA considers that as part of the nonclinical package, a single adequately designed GLP-compliant 3-month toxicity study can be sufficient to evaluate *in vivo* safety and support first in human dosing. Herein, we summarize the nonclinical safety findings from four 13-week rat repeat dose studies sponsored by the n-Lorem Foundation for the treatment of nano-rare neurologic diseases. Rats were dosed monthly via intrathecal lumbar bolus injection with a vehicle or ASO on Study Days 1, 29, 57, and 85 and euthanized on Day 92. Animals were evaluated for a comprehensive list of in-life and post-mortem endpoints. The brain and spinal cord showed dose dependent ASO accumulation. ASO-related functional and neurobehavioral effects were transient, resolving within 24-hours of dosing, and most often consisted of minimally to slightly impaired/abnormal gait. Microscopic findings were largely secondary to the uptake and accumulation of ASO by macrophages and renal tubule epithelial cells or minimal leukocyte infiltrates in response to ASO. None of these findings were considered adverse, and human patients were successfully dosed without any adverse events.

## P38 Absolute Quantitation vs. Semi-Quantitative Analysis of Expression of Biomarkers Using Image Analysis Software

Sasmita Mishra<sup>1</sup>, Tyler Peat<sup>1</sup>, Victoria Arndt<sup>2</sup>, Susan Lynk<sup>2</sup>, Steve Van Adestine<sup>2</sup>, Pamela Blackshear<sup>1</sup>

<sup>1</sup>Labcorp, Greenfield, IN, USA. <sup>2</sup>Labcorp, Madison, WI, USA.

### Abstract

**Introduction:** Expression of proteins/mRNAs can be quantitated semi-quantitatively using a microscope or digitized images. The output is presented as minimal, slight, moderate, marked, or severe, which can be converted to minimal (1-20%), slight (11-25%), moderate (26-50%), marked (51-75%), or severe (76-100%). However, using image analysis software, the percent can be presented precisely. The analysis is based on area quantification, cell-based measurements (membrane, cytoplasm, or nuclear), or object-based quantification using image analysis algorithms. **Methods:** The tissues were stained with various antibodies for image analysis; heart with Frataxin, brain with GFAP, kidney with alpha-2 macroglobulin, spleen, and tonsils with CD3, CD4, CD8, CD19, CD20 antibodies for T or B lymphocytes either individually or in combination (multiplexing). **Results:** Area quantification for Frataxin, GFAP, alpha-2 macroglobulin were precise and resulted in various intensity of staining with % area positive. The cell-based analysis for all lymphoid tissues resulted in % cells positive with various intensities. Additionally, multiplexing of lymphoid tissues determined the location of various population. Muscle fiber diameter algorithm measured the average diameter of muscle fibers for the whole tissue with detailed information about individual muscle fiber diameter. **Conclusion:** This study compared various image analysis algorithms with semiquantitative analysis for more precise results leading to appreciation of the use of image analysis algorithms for any efficacy/toxicity studies. Area quantification algorithm can be used for more extensive expression of biomarkers, cell-based algorithms can be used in oncology for quantitation of tumor cells or inflammatory cells, and muscle fiber algorithms for muscular dystrophy syndrome models.

## P39 Deep Learning-Based Method for Anatomical Subsite-Wise Evaluation of Single Cell Necrosis and Vacuolation of Neuron/Nerve Fiber of CNS Toxicity in Rats

Taishi Shimazaki<sup>1</sup>, Yuzo Yasui<sup>1</sup>, Kyotaka Muta<sup>1</sup>, Naohito Yamada<sup>1</sup>, Amogh Mohanty<sup>2</sup>, Aashay Tinaikar<sup>2</sup>, Rohit Garg<sup>2</sup>, Tijo Thomas<sup>2</sup>, Toshiyuki Shoda<sup>1</sup>

<sup>1</sup>Japan Tobacco Inc., Yokohama, Japan. <sup>2</sup>AIRA Matrix, Mumbai, India.

### Abstract

**Introduction:** Assessment of changes within the central nervous system (CNS) including single cell necrosis and vacuolation of neuron/nerve fiber is a sensitive method to assess toxicity. A deep learning-based algorithm for analysis of single cell necrosis and vacuolation is proposed for 7 levels of rat brain.

**Materials and Methods:** Six-week-old male Sprague-Dawley rats, that were necropsied after a single or repeated 4-day administration of vehicles or compounds inducing CNS toxicity, used in this study. The WSIs of each level of the brain sections of the subjects were divided into training sets and test sets. For training the deep learning models, we selected 1024x1024 sized tiles at 40x magnification for single cell necrosis and vacuolation of neuron/nerve fiber; and 2048x2048 sized tiles at 2.5x magnification for region segmentations across 7 levels of rat brain. After training, performance of the algorithm was evaluated using the WSIs in the test set which were obtained from rats treated with neurotoxicity-inducing compounds. The performance of the algorithm was further improved by repeatedly additional validation and re-training.

**Results:** The algorithm demonstrated high sensitivity and specificity values in detecting these findings, and generally correlated with the histopathological diagnosis given by JSTP-qualified pathologists.

**Conclusion:** This model was able to perform an anatomical subsite wise analysis of single cell necrosis and vacuolation of neuron/nerve fiber in 7 levels of rat brain. This method can be used as an adjunctive function in pathologists' histopathological evaluation, for CNS toxicity screening in early non-GLP toxicity studies.

## P40 Deep Learning Solution for the Automated Assessment of the Rodent Thymus

Rajesh Ugalmugle<sup>1</sup>, Deb Tokarz<sup>2</sup>, Dev Kumar Das<sup>1</sup>, Gunjan Deotale<sup>1</sup>, Tijo Thomas<sup>1</sup>, Uttara Joshi<sup>1</sup>

<sup>1</sup>AIRA Matrix, Mumbai, India. <sup>2</sup>Experimental Pathology Laboratories, Inc., Durham, NC, USA.

### Abstract

**Introduction:** Thymus, being a primary lymphoid organ, is a sensitive target following exposure to immunotoxins. Reduction in cortical lymphocytes is an important histopathological finding in compound-induced effects. Hence evaluating the cortico-medullary ratio, and assessing the cortical lymphocytes is important. Manual histopathological assessment of these features can be a time-consuming process with subjective outputs. We developed a deep-learning solution for the automated assessment of the rodent thymus. The solution separately identifies the cortex and medulla, computes the cortico-medullary ratio, and quantifies lymphocytes and apoptotic cells in each compartment.

**Materials and Methods:** WSIs of 320 H&E-stained Wistar rat thymus sections from seven sources were used. Training patches were generated from 240 WSI, while the remaining 80 WSIs were retained for blind testing. Separate U-Net segmentation architectures were trained to segment the medulla, cortex, lymphocytes, and apoptotic cells.

**Results:** The DICE scores (F1-scores) were: 94% for the cortex, 98% for the medulla, 85% for apoptosis, and 88% for lymphocytes. The trained model achieved a precision of 97% and recall of 91% averaging over four parameters when compared with pathologist's observations.

**Conclusion:** The proposed deep-learning solution can accurately segment and quantify cortex and medulla as well as detect and quantify lymphocytes and apoptotic cells. This solution can be used as a supportive tool for detecting decreased cortical lymphocyte cellularity in the thymus.

**Impact statement:** This solution has the potential to be used as an adjunct in the enhanced histopathological evaluation of the thymus.

## P41 AI-Based Approach for Quantifying and Grading Bile Duct Hyperplasia in Mice

Ingeborg M. Langohr<sup>1</sup>, Dayananda Siddappa Thimmanahalli<sup>1</sup>, Nathan Pate<sup>2</sup>, Dinesh S. Bangari<sup>1</sup>, Dev Kumar Das<sup>3</sup>, Kuldeep Gautam<sup>3</sup>, Arshad Kazi<sup>3</sup>, Tijo Thomas<sup>3</sup>, Uttara Joshi<sup>3</sup>, Rajesh Ugalmugle<sup>3</sup>

<sup>1</sup>Global Discovery Pathology, Translational Models Research Platform, Sanofi, Cambridge, MA, USA. <sup>2</sup>Charles River Laboratories, Reno, NV, USA. <sup>3</sup>AIRA Matrix, Mumbai, India.

### Abstract

**Background:** Bile duct hyperplasia in rodents can represent a direct or indirect effect of chemicals by cytotoxicity or interference with bile flow, respectively. It may also be observed as a spontaneous change in portal areas of older animals. We developed an AI model to for accurate severity assessment of bile duct hyperplasia in rodents.

**Materials and Methods:** H&E-stained mice liver sections from two studies digitized using an Aperio GT 450 scanner (Study 1) and Leica Aperio AT2 scanner (Study2).

### Model Development

- 1165 patches of size 1024x1024 pixels from 35 WSI extracted at 20x magnification (Study1)
- Patches used to train a deep learning-based model to identify bile ducts using a Unet architecture with an EfficientNet backbone.
- The quantitative output provided by the model included the count & percentage area occupied by bile ducts.
- Clustering was performed to further categorize into four groups to indicate the severity of bile duct hyperplasia.
- The model was validated for performance at WSI level using 24 withheld WSI from Study1.

### Model Testing

The validated model was then tested on 68 WSI from Study2.

### Results

#### Model Development:

- Dice scores for bile duct segmentation model on training and validation sets: 91.75% and 85.88%, respectively.
- Model validation on WSI: sensitivity: 95%, specificity: 97%

#### Testing:

High correlation of cluster-based severity categories in comparison with the grading provided by 3 veterinary pathologists.

#### Conclusions & Impact Statement

The AI model provides a sensitive and specific method for bile duct quantification and can be used as an adjunct for assessing bile duct hyperplasia in mice.

## P42 Development and Evaluation of HALO and HALO AI Image Analysis Tools for Quantitative Histopathology Scoring of Lung Pathology in Experimental Tuberculosis Infections of Rhesus Macaques

*Vinay Shivanna, Olga Gonzalez, Edward J. Dick, Jr.*  
Texas Biomedical Research Institute, San Antonio, TX, USA.

### Abstract

Image analysis platforms have become very popular for their ability to conduct high-throughput, multiplex, and quantitative analyses of a wide range of tissues. However, analysis of tissues with dynamic morphology such as the lung remains challenging. Variability in lung collection and fixation methods leads to variable appearance of histology with compressed lung demonstrating the crowded appearance of anatomic structures. The dynamic histologic appearance of the lung also poses a complex challenge for image analysis platforms to differentiate and predict the normal vs areas of inflammation. Well-trained algorithms should be a faster way to detect and quantify the areas of pathology with greater consistency and efficiency.

One-hundred, H&E stained slides were selected from different rhesus macaques that were experimentally infected with *Mycobacterium tuberculosis* which produces varying degrees of pathology primarily characterized by granuloma formation. Here, we used a random forest tissue classifier (HALO®) and a DenseNet V2 AI classifier module (HALO AI) that board-certified pathologists trained independently to identify granulomas and calculate the percentage of lung affected. Further, the classifier modules were also trained to detect and quantify different granuloma components, primarily the areas of necrosis, cellular wall, and the peripheral lymphocytic aggregate.

HALO AI, the Deep Learning Classifier Add-on that was trained by pathologists, performed significantly better than the random forest classifier in detecting and quantifying granuloma areas and also the different granuloma components. With further extensive validation, this HALO AI-trained module can be used to automate histopathology scoring of lung tissues for assessing pathology associated with tuberculosis.

## P43 Solving the Reference Pathologist Paradox in Machine Learning Development for Histology Scoring

*Thomas Forest<sup>1</sup>, Sabu Kuruvilla<sup>1</sup>, Binod Jacob<sup>1</sup>, Nagaraja Muniappa<sup>1</sup>, Takayuki Tsuchiya<sup>1</sup>, Raymond Gonzalez<sup>1</sup>, Malini Roy<sup>2</sup>, Raghav Amaravadi<sup>2</sup>, Geetank Raipuria<sup>2</sup>, Nitin Singhal<sup>2</sup>*  
<sup>1</sup>Merck & Co., Inc., Rahway, NJ, USA. <sup>2</sup>Aira Matrix, Mumbai, India.

### Abstract

**Introduction** – Development of machine learning (ML) algorithms for scoring histology slides commonly involves training against example histopathology findings. This approach creates a ML performance boundary based on the list of diagnoses included and the observations recorded by the reference pathologists. We hypothesized that a ML development strategy not requiring training against histopathology findings could increase algorithm performance.

**Design** – Two ML algorithms were developed for scoring Han Wistar rat kidney histology. ML scoring was compared to the independent evaluations of 3 experienced toxicologic pathologists using a rat study of carbapenem, a classical renal toxicant.

**Results** – Scores from the ML trained using examples of renal tubular histopathology aligned closely with the consensus of the pathologist panel. Whereas scores from a ML trained only using histology from vehicle treated rats identified a subtle histomorphology difference in a dose group anticipated to be not remarkable based on previous studies and considered not remarkable by the consensus of the pathologist panel.

**Conclusion** – A ML algorithm that scored histology based on deviation from a model of normal histomorphology identified a subtle non-adverse difference between control and treated groups that ML trained using histopathology examples did not identify. These differences were not considered toxicologically noteworthy by a panel of experienced pathologists.

**Impact** – Advances in ML development for scoring histology slides introduce a novel frontier for detecting subtle histomorphology differences in nonclinical toxicology studies that may need to be incorporated into risk assessments in future workflows.

## P44 Congenital Thyroid Dysplasia in C57BL/6NTac Due to LINE Transposition into Thyroglobulin Gene

Thomas Forest<sup>1</sup>, Wendy Bailey<sup>1</sup>, Bart Smits<sup>2</sup>, Zoltan Erdos<sup>1</sup>, John Gaspar<sup>1</sup>, Warren Glaab<sup>1</sup>, Sabu Kuruvilla<sup>1</sup>, Pamela Lane<sup>1</sup>, Thomas Rosahl<sup>1</sup>, Douglas Thudium<sup>1</sup>, Jingzhou Wang<sup>1</sup>, Melissa MacGowan<sup>2</sup>, Heather Multari<sup>2</sup>, Christine Cumo<sup>2</sup>, Adam Navis<sup>2</sup>

<sup>1</sup>Merck & Co., Inc., Rahway, NJ, USA. <sup>2</sup>Taconic Biosciences, Germantown, NY, USA.

### Abstract

**Introduction/Objectives** – Thyroid dysplasia was identified during routine phenotyping of a genetically modified mouse line generated in the C57BL/6NTac background. Further histologic characterization of wildtype C57BL/6NTac identified thyroid dysplasia in stock mice. An investigation was undertaken to determine the underlying genetic cause and develop DNA-based test to eliminate the mutation from the Taconic colony.

**Experimental Design/Methods and Materials** – Wildtype C57BL/6NTac mice with and without thyroid dysplasia were characterized by light microscopy, transmission electron microscopy, and immunohistochemistry. Body weight, body temperature, heart rate, thyroid stimulating hormone and thyroid hormone levels were measured. Thyroglobulin (TG) mRNA was extracted and sequenced. Whole genome DNA sequencing was performed.

**Results** – No alterations were observed in body weight, temperature, or heart rate. DNA sequencing identified a LINE transposition into the intron adjacent to exon 26 of TG, which modulated splicing of exon 26 during RNA transcription, resulting in aberrant TG translation, accumulation of TG in the endoplasmic reticulum of thyroid epithelial cells, decreased T4 levels, increased TSH, and proliferation of thyroid epithelial cells leading to adenoma formation by 9 months of age.

**Conclusion** – A LINE transposition was identified as a cause of thyroid dysplasia in wildtype C57BL/6NTac mice.

**Impact Statement** – Identifying the DNA change responsible for thyroid dysplasia in C57BL/6NTac mice enabled development of a DNA test used to eliminate the mutation from the stock mouse colony.

## P45 Safety Assessment of Repeated Intra-Articular Injections of pMPCylated Liposomes in Rat Models for Knee Osteoarthritis Therapy

Yuval Ramot<sup>1,2</sup>, Noam Kronfeld<sup>3</sup>, Michal Steiner<sup>4</sup>, Eric D. Lee<sup>5</sup>, Ronit Goldberg<sup>6</sup>, Sabrinal Jahn<sup>6</sup>, Abraham Nyska<sup>7,8</sup>

<sup>1</sup>Faculty of Medicine, Hebrew University of Jerusalem, Jerusalem, Israel. <sup>2</sup>Department of Dermatology, Hadassah Medical Center, Jerusalem, Israel. <sup>3</sup>HBI Biotech Sciences Ltd, Ness-Ziona, Israel. <sup>4</sup>Preclinical consultant, Rehovot, Israel. <sup>5</sup>StageBio, Frederick, MD, USA. <sup>6</sup>Liposphere Ltd., Givat-Shmuel, Israel. <sup>7</sup>Consultant in toxicologic pathology, Tel Aviv, Israel. <sup>8</sup>Tel Aviv University, Tel Aviv, Israel.

### Abstract

Knee osteoarthritis (OA) presents a substantial healthcare challenge. This study evaluates the safety of repeated intra-articular injections of the pMPCylated liposomal boundary lubricant AqueousJoint, a novel, mechanically-acting, therapeutic approach for knee OA. Two experiments were conducted on Sprague-Dawley rats, involving 2 or 3 intra-articular injections of AqueousJoint. The rats were observed for 1 or 13 weeks post the last injection, with assessments including clinical, histopathological, and immunohistochemical evaluations. No mortality or abnormal clinical signs were observed. Histopathology indicated minimal vacuolated macrophages, predominantly M2-like, suggesting a non-adverse response. Immunohistochemistry supported the predominance of M2-like macrophages. Statistical analysis showed no significant differences in body weight, clinical pathology, or organ weights compared to controls, affirming the safety of repeated intra-articular pMPCylated liposome injections. The study confirms the safety of repeated intra-articular injections of pMPCylated liposomes in rat models, supporting its potential as a biocompatible solution for knee OA therapy, offering a promising avenue for future clinical applications.

**P46 Effects of the Pharmacological YAP-TEADs Inhibitor Verteporfin in Preovulatory Bovine Granulosa Cells Viability**

*Esdras Correa dos Santos<sup>1</sup>, Christopher Price<sup>2</sup>, Gustavo Zamberlam<sup>2</sup>*

<sup>1</sup>University of Georgia, Athens, Georgia, USA. <sup>2</sup>Universite de Montreal, Saint Hyacinthe, Quebec, Canada.

**Abstract**

Cystic ovarian disease (COD) in dairy cattle is characterized by preovulatory follicles that fail to ovulate and persist in the ovary. Recently, we found that protein levels for the Hippo pathway effector YAP and its classic transcriptional activators TEADs are significantly higher in ovarian granulosa (GCs) isolated from cystic follicles. These findings indicate that the classic YAP-TEADs binding pharmacological inhibitor Verteporfin (VP) represents a potential new treatment for COD. However, before testing *in vivo* VP effects on follicle cysts, we decided to determine *in vitro* whether VP treatment can alter preovulatory GCs function and apoptosis.

Bovine GCs from  $\geq 10$  mm diameter follicles were cultured with distinct doses of VP (1  $\mu$ m and 5  $\mu$ m) for 6, 12 and 24h. mRNA abundance was measured by real-time qPCR.

To confirm VP specificity, we measured mRNA levels for classic YAP-TEAD target genes *CTGF* and *CYR61* which were significantly downregulated by the two doses of VP in all time points tested ( $P < 0.05$ ). While VP did not alter the mRNA basal levels of the classic preovulatory gene *EREG* ( $P > 0.05$ ), VP increased in a dose-dependent manner the expression of LH receptor (*LHCGR*) at 24h ( $P < 0.05$ ). Although VP treatment did not alter mRNA levels for P53 and BAX, two proapoptotic genes ( $P > 0.05$ ), VP treatment seems to stimulate the mRNA levels for *BCL2*, an antiapoptotic protein ( $P < 0.05$ ).

YAP-TEAD binding inhibition by Verteporfin does not seem to affect bovine GCs viability *in vitro*. These preliminary findings suggest that the use of VP in intrafollicular injections *in vivo* may represent a specific potential treatment for COD.

**P47 A SARS-CoV2 mRNA Vaccine Candidate (CUK3-1/LNP128) Induces Reversible Bone Marrow Suppression in ICR Mice**

*Jae-Hun Ahn<sup>1</sup>, Na-Young Lee<sup>2</sup>, Hee-Jin Bae<sup>1</sup>, Euna Kwon<sup>1</sup>, Gyochang Keum<sup>3</sup>, Jae-Hwan Nam<sup>4</sup>, Byeong-Cheol Kang<sup>2</sup>*

<sup>1</sup>Seoul National University Hospital, Seoul, Republic of Korea.

<sup>2</sup>Seoul National University, Seoul, Republic of Korea. <sup>3</sup>Korea Institute of Science and Technology, Seoul, Republic of Korea.

<sup>4</sup>The Catholic University of Korea, Bucheon, Kyonggi-do, Republic of Korea.

**Abstract**

**Introduction:** SARS-CoV2 mRNA vaccine-induced side effects have been extensively reported in the clinical field. However, the potential toxicity of mRNA vaccines has not been fully identified. We aimed to clarify mRNA vaccine-induced toxicity. **Experimental Design:** Six-week-old CrIOr:CD1(ICR) mice were used. CUK3-1/LNP128, a SARS-CoV2 S protein coding nucleoside-modified mRNA vaccine candidate, was injected intramuscularly (IM) or intravenously (IV) twice at 2-week intervals (100 ug/head). **Methods:** Necropsy was performed at 2- or 14-day post-secondary injection (dpi). Blood and serum parameters were determined by CBC or ELISA. Histopathological changes were evaluated by H&E stain. Gene expression in bone marrow was analyzed by RNA sequencing. **Results:** IM injection of CUK3-1/LNP128 sufficiently induced S protein-specific IgG. Notably, CUK3-1/LNP128 induced significant decrease of erythroid cells in bone marrow at 2 dpi. CUK3-1/LNP128-induced bone marrow suppression was mediated by the complete mRNA vaccine, but not by mRNA only or LNP only. Interestingly, IV injection of CUK3-1/LNP128 with same dosage (100 ug/head) also induced bone marrow suppression at comparable level to IM injection. Importantly, S protein non-coding/luciferase-coding mRNA vaccine also induced bone marrow suppression. In addition, the CUK3-1 sequence was detected in bone marrow tissue of CUK3-1/LNP128-injected mice and several cell death-related genes were upregulated in bone marrow tissue. However, bone marrow suppression was recovered at 14 dpi. **Conclusion:** We confirmed that mRNA vaccine can cause toxicological changes in bone marrow tissue. **Impact statement:** Although the underlying mechanism needs to be clarified, our findings suggest that mRNA vaccine-induced bone marrow toxicity should be cautiously considered in the pre-clinical developmental process.

## P48 Development-Limiting Toxicity Associated with a Dual Targeting Bispecific T-Cell Engager in a 28-Day Nonhuman Primate Toxicology Study

*Joan H. Lane<sup>1</sup>, Rhian Prunicki<sup>2</sup>, Rodolfovan Yabut<sup>2</sup>, William Siska<sup>3</sup>, Christine Mollica<sup>4</sup>*

<sup>1</sup>Amgen, Cambridge, MA, USA. <sup>2</sup>Amgen, San Francisco, CA, USA.

<sup>3</sup>Charles River Laboratories, Reno, NV, USA. <sup>4</sup>Amgen, Thousand Oaks, CA, USA.

### Abstract

**Introduction/Objectives** AMGXXX is dual targeting “or” BiTE® (Bispecific T-cell Engager) intended to treat certain cancers by binding one or both target cell surface proteins and directing tumor cell lysis via CD3 engagement and activation of T cells. **Experimental Design** An IND-enabling toxicology was initiated in cynomolgus monkeys. On Days 1, 3, and 5, AMGXXX-treated groups were equally “step-dosed” at 2.5, 5, and 25 ug/kg to attenuate possible adverse cytokine release. On Days 8-29, Groups 2, 3, and 4 were to receive weekly doses of 25, 50 or 125 ug/kg, respectively. Standard toxicology endpoints and repeated serum cytokine measurements were evaluated. **Results** AMGXXX was poorly tolerated in all groups with gastrointestinal signs and general debility resulting in unscheduled deaths on Day 8-11. Serum IL-6 and MCP1 levels, which are typically attenuated with repeat dosing of BiTE® molecules, showed escalating elevations. Clinical pathology findings were consistent with an acute phase response. Organ weight changes included increased adrenal gland and spleen weight and decreased thymic weight. AMGXXX-specific light microscopic findings were limited to perivascular hemorrhage in the paracortices of lymph nodes. Investigative immunohistochemistry revealed an increase in drug target staining intensity in endothelial cells and macrophages within lymph nodes and the intestinal lamina propria. **Conclusion, Impact Statement** Data analyses indicated moribundity was associated with a cytokine response that did not attenuate with step dosing. These changes correlated with an apparent dose-dependent upregulation of target expression demonstrated by immunohistochemistry.

## P49 Use of Virtual Control Groups in Nonhuman Primate Ocular Nonclinical Toxicity Studies

*Oliver C. Turner<sup>1</sup>, Clare Thomas<sup>2</sup>, Christopher Hayden<sup>2</sup>, Johann Mueller<sup>3</sup>, Helen Booler<sup>3</sup>*

<sup>1</sup>Novartis, East Hanover, NJ, USA. <sup>2</sup>Novartis, Cambridge, MA, USA.

<sup>3</sup>Novartis, Basel, Switzerland.

### Abstract

An area of active exploration to implement the 3Rs and decrease the number of animals used in research, is the concept of the Virtual Control Group (VCG) for nonclinical toxicity studies. In this work, we developed and tested the feasibility and utility of the VCG approach within the specific context of ocular drug development. Non-human primates (NHP) are commonly selected for the development of ocular therapeutics because of anatomical and physiologic similarities with human eyes, but ethics, availability and cost make attempts to decrease the numbers used particularly relevant. However, with invasive ocular routes of administration, procedure-related findings are common, and must be understood to differentiate from test article-related effects.

Using archived whole slide images, a searchable virtual control database (VCD) within Patholytix Study Browser (v2.2.0.20) (Deciphex™) was assembled with 668 whole-slides images (from 36 studies) of control non-human primate eyes from ocular and standard non-ocular toxicity studies.

Easy searchability enabled rapid assessment and comparison of procedure-related histopathology findings in studies using the virtual control eyes, replacing (in the context of non-pivotal studies), or supporting utilization of smaller concurrent controls. A large VCD proved much quicker to search (by sex, species, study duration, route of administration etc.) and more versatile than the glass repository.

The authors believe that in the context of ocular toxicologic pathology, VCGs can improve sensitivity and aid decision making, enabling the reduction or replacement of concurrent controls in non-pivotal NHP ocular toxicology studies.

## P50 Background Findings of Infrequently Examined Bones in Beagle Dogs

*Phaedra J. Cole*<sup>1</sup>, *Agathe Bédard*<sup>2</sup>, *Sara Tonissen*<sup>3</sup>  
<sup>1</sup>Zoetis, Kalamazoo, MI, USA. <sup>2</sup>Charles River Laboratories, Senneville, Quebec, Canada. <sup>3</sup>The Ohio State University, Columbus, OH, USA.

### Abstract

**Introduction:** Bone evaluation for standard dog toxicology studies generally includes one section through the femur, tibia, rib, sternum, and/or tibio-femoral joint.

In studies with enhanced bone and joint histopathology, additional sections through the tibia and ulna revealed background findings that had not been previously reported. Understanding background findings is essential to interpret findings in treated animals on safety studies accurately.

**Design:** Data includes control Beagle Dogs from two safety studies (15) and Age-Matched, Naïve Beagle dogs (6). Tibial plateaus were sectioned in 3 midsagittal planes. Proximal ulna was bisected midsagittally. Sections were stained with H&E and toluidine blue for proteoglycan evaluation. Other bones (proximal/distal femur, acetabulum, humerus, scapula, and/or proximal radius) were processed and evaluated.

**Results:** Focal to regionally extensive, generally bilateral, cartilage degeneration was observed within the ulna of the study control (3 of 15) and Naïve (4 of 6) dogs. Degeneration was variably accompanied by erosion, necrosis, and/or proteoglycan depletion.

Focal or multifocal and bilateral cartilage degeneration and proteoglycan depletion were noted in the proximal tibia of control and Naïve dogs. The degeneration was typified by surface irregularity/fibrillation associated with depletion of proteoglycan staining noted with toluidine blue staining.

No significant microscopic findings were noted in other bones evaluated.

**Impact Statement:** This report describes findings in the proximal ulna and tibia of control and naïve laboratory Beagle dogs. Understanding and recognizing background findings in bones is essential to interpret possible test article-related findings in toxicology studies including enhanced bone and joint histopathology.

## P51 Retrospective Review of Histopathology Findings in Beagle Dogs in Powder Inhalation Toxicology Studies

*Predrag Novakovic*, *Joseph Younan*, *William Lee*, *Kevin McNally*, *Lev Kolodzieyski*, *Stephen Groom*  
 ITR Laboratories Canada Inc., Baie D'Urfe, Quebec, Canada.

### Abstract

**Introduction:** Inhalation drug market is one of the fastest growing in the pharmaceutical industry. Due to the increased use of different types of powder carriers with various physicochemical properties in the drug delivery formulations, there is an increasing need for the establishment of baseline levels of histopathological findings in the respiratory system of dogs in inhalation toxicology studies.

**Experimental Design:** Beagle dogs receiving vehicle control item from 41 powder inhalation studies conducted at ITR Laboratories Canada between 2008 and 2023 were retrospectively reviewed for histopathological findings at all levels of respiratory tract.

**Methods:** Provantis software was used to determine incidence and severity of microscopic findings. **Results:** The overall incidence of histopathological findings in respiratory tissues from powder control dogs was 19% compared to 15% in air control dogs. Most common findings in powder control dogs consisted of minimal increase in alveolar macrophages (15%) along with minimal alveolar inflammatory cells infiltrates (13%) in the lungs. These findings were observed in 29% of non-lactose powder blend treated controls compared to 12% lactose-based powder treated controls. **Conclusion:** Differences in the incidence of histopathological findings in the lungs were observed between powder treated and air control dogs. Severity of findings in the respiratory tract was comparable between powder and air control animals. Differences in the incidence of findings were observed between control dogs treated with different powder blends. **Impact statement:** These results will be used to determine baseline levels of microscopic findings in respiratory tract of dogs treated with most common powder carriers.

## P52 Procedure-Related, Artifact, and Spontaneous Background Microscopic Findings in Eyes from African Green Monkeys (*Chlorocebus sabaeus*) Used in Ocular Toxicology Studies

*Rahul B. Dange, Jennifer Cann, Richard Bouffard, Melissa Miles, Emily Ramirez, Nadine Swierzawski, Matthew Lawrence*  
Virscio, New Haven, CT, USA.

### Abstract

**Introduction:** To precisely and confidently identify microscopic findings associated with test article (TA) administration in ocular toxicology studies, the anatomic pathologist needs to be aware of any procedure-related, spontaneous, or artifactual changes that may also be seen. **Methods:** The purpose of this study is to describe frequently observed procedural, artifactual, or spontaneous background findings in archived globes from control and treated (lacking TA-related findings) African Green Monkeys (AGM) used in preclinical ocular toxicology studies. **Results and conclusion:** Commonly noted procedure-related findings consisted of separation of neuroretina from the retinal pigment epithelium (RPE), RPE hypertrophy, hyperplasia and migration in to the neuroretina, erosion/hyperkeratosis of the corneal epithelium, atrophy of the outer nuclear layer, focal atrophy with disruption of the retina, fibroplasia and neovascularization of choriocapillaris and nerve fiber degeneration in the optic nerve due to experimental laser injury, and lymphoplasmacytic and histiocytic uveitis due to anterior segment cannulation. Separation of sclera from the choroid, RPE separation from the neuroretina without RPE hypertrophy, vacuolation of the outer plexiform layer, and optic nerve vacuolation were frequent artifactual findings associated with the collection, fixation, and processing procedures. Commonly observed background findings included peripheral displacement of photoreceptor nuclei, eosinophilic inclusions in the inner photoreceptor layers, and mononuclear cell infiltrates in the cornea, ciliary body, and conjunctiva. **Impact statement:** Procedural, artifactual, or spontaneous background findings in eyes from AGM will help prevent misinterpretation of these findings as TA-related, affecting study conclusions.

## P53 Procedure-Related, Artifact, and Spontaneous Background Microscopic Findings in Central Nervous System and Dorsal Root Ganglion from African Green Monkeys (*Chlorocebus sabaeus*) Used in Neurotoxicology Studies

*Rahul B. Dange, Jennifer Cann, Richard Bouffard, Melissa Miles, Emily Ramirez, Golnaz Jalalahmadi, Matthew Lawrence*  
Virscio, New Haven, CT, USA.

### Abstract

**Introduction:** To produce accurate and reproducible histopathology data for preclinical toxicology studies, anatomic pathologists need to know the procedure-related, spontaneous, and artifactual microscopic findings that may be present in order to precisely distinguish them from findings associated with administration of a test article (TA). **Methods:** The purpose of this study is to present these frequently observed findings in the central nervous system (CNS) and dorsal root ganglion (DRG) of control and treated (lacking TA-related findings) African Green Monkeys (AGM) used in preclinical neurotoxicology studies. **Results and conclusion:** Common procedure-related findings included nerve fiber degeneration within the dorsal funiculus of spinal cord segments, brainstem, and cerebellum; and meningeal fibrosis with mononuclear cell infiltration in AGM receiving TA or control via intrathecal (IT) or intra-cisterna magna (ICM) routes. Procedure-related multifocal ischemic necrosis within the subpial cerebrum with hemorrhage was also noted in a surgical AGM model of ischemic stroke. Pronounced widespread vacuolation of the white matter, and less commonly gray matter, of the brain, spinal cord, and optic nerve was a frequent artifactual finding associated with collection, fixation, and processing of tissues. Commonly observed background findings included mononuclear cell infiltration within the meninges of spinal cord, brain, and DRG, focal mineralization in brain and DRG, intracytoplasmic inclusions in DRG neurons, pigment in neurons, and melanomacrophages in the brain, DRG, and meninges. **Impact statement:** Procedural, artifactual, or spontaneous background findings in CNS and DRG of AGM will help prevent misinterpretation of these findings as TA-related.

## P54 Pathology Associated with Human CAR T Cell in NSG Mice: A Retrospective Review

*Renata M. Mammon<sup>1</sup>, Alessandra Piersigilli<sup>2</sup>, Ileana C Miranda<sup>1</sup>*

<sup>1</sup>Laboratory of Comparative Pathology, Memorial Sloan Kettering Center, Weill Cornell Medicine, and The Rockefeller University, New York, NY, USA. <sup>2</sup>Department of Drug Safety Research and Evaluation, Takeda Development Center Americas, Cambridge, MA, USA.

### Abstract

Chimeric antigen receptor (CAR) therapy has been a promising treatment for neoplasia and autoimmune disease. Immunocompromised mice are a common model to test efficacy and safety of CAR T cells of human origin. Preclinical toxicity associated with CAR T cell products encompasses a spectrum of morphologic changes with currently limited literature documentation. Xenogeneic graft-versus-host disease (xGvHD), aberrant proliferation of human T cells with tissue invasion, macrophage activation syndrome (MAS), vasculitis and thrombosis were the lesions associated with toxicity in immunodeficient NOD.Cg-Prkdc<sup>scid</sup>Il2rg<sup>tm1Wjl</sup>/SzJ (NSG) and NOD.Cg-Prkdc<sup>scid</sup> Il2rg<sup>tm1Wjl</sup> Tg(CMV-IL3,CSF2,KITLG)1Eav/MloySzJ (NSG-SGM3) mice submitted to the Laboratory of Comparative Pathology (LCP) at Memorial Sloan Kettering Cancer Center. The purpose of this retrospective study is to review the histopathologic lesions and toxicity associated with human CAR T cells in NSG and NSG-SGM3 mice submitted to the LCP from 2019 till present. The hypothesized pathogenesis and translatability of the toxicity for each condition are discussed.

## P55 Investigation of Human and Bovine Thrombin-Effects on Cynomolgus Monkey Platelets and Evaluation of a Monoclonal Antibody Specific for Human Thrombin Receptor

*Florence M. Poutout-Belissent<sup>1</sup>, Anthony Pincon<sup>1</sup>, Weizhen Wu<sup>2</sup>, Katheryne Larocque<sup>1</sup>, Lori Morton<sup>2</sup>, Dan Chalothorn<sup>2</sup>*

<sup>1</sup>Charles River Laboratories, Senneville, QC, Canada. <sup>2</sup>Regeneron Pharmaceuticals Inc., Tarrytown, NY, USA.

### Abstract

**Introduction:** Thrombin is a potent agonist of platelet aggregation. Thrombin receptors are protease-activated receptors (PARs) present on platelets 'membrane. Bovine  $\alpha$ -thrombin is known to bind human platelets with a higher affinity than human  $\gamma$ -thrombin. We investigated the effect of  $\alpha$ - and  $\gamma$ -thrombin on cynomolgus monkey platelets to study a monoclonal antibody (mAb) targeting platelet function.

**Methods:** Human  $\gamma$ -thrombin and bovine  $\alpha$ -thrombin were spiked in monkey platelet rich plasma (PRP) at 50-750 nM, and in human washed platelets at 58-470 nM and 0.68-5.44 nM respectively. Platelet aggregation was monitored on PAP8E and Chrono-log aggregometers. An anti-PAR mAb was spiked in monkey PRP samples at 3-100 nM and human washed platelets at 19-75 nM with optimal concentrations of  $\gamma$ - and  $\alpha$ -thrombin to evaluate the mAb inhibition of thrombin-mediated platelet aggregation.

**Results:** Platelet aggregation with bovine  $\alpha$ -thrombin was optimal at concentrations  $\geq$  50 nM in monkey samples, at 1.36 to 5.44 nM in human samples, with human  $\gamma$ -thrombin at 500-750 nM in monkey samples and at 235-470 nM in human samples. Anti-PAR mAb inhibited aggregation with  $\gamma$ -Thrombin in monkey PRP at 500 nM and human washed platelets at 19 nM. The anti-PAR mAb had no effect on monkey and human platelet aggregation induced with bovine  $\alpha$ -Thrombin at any dose tested.

**Conclusion:** The high affinity of an anti-PAR mAb to human  $\gamma$ -thrombin platelet receptors was demonstrated by comparing platelet aggregation induced with human  $\gamma$ -thrombin or bovine  $\alpha$ -thrombin on human and monkey platelets. In cynomolgus monkey and human,  $\gamma$ - and  $\alpha$ -thrombin bind different platelet receptors.

## P56 Investigation of Compound-Related Effects on Fibrinolysis with a Microplate Turbidimetric Fibrinolytic Assay

Anthony Pincon<sup>1</sup>, Florence M. Poitout-Belissent<sup>1</sup>, Tetyana Redko<sup>1</sup>, Marc-Olivier Pepin<sup>1</sup>, Dorothy Flood<sup>2</sup>, Tom J. Parry<sup>2</sup>

<sup>1</sup>Charles River Laboratories, Senneville, QC, Canada.

<sup>2</sup>NeuroTrauma Sciences, LLC, Alpharetta, GA, USA.

### Abstract

**Introduction:** Fibrinolysis plays an important role in regulating thrombosis by facilitating clot dissolution. Given the widespread use of thrombolytics in ischemic indications, it is important to evaluate compound pharmacodynamic drug-drug interactions (PD-DDI) with fibrinolytics. We developed a turbidimetric fibrinolytic assay to study potential PD-DDI on tissue plasminogen activator (tPA) and tenecteplase (TNK) of a neurosteroid, NTS-105, being developed for use in acute ischemic stroke.

**Methods:** Pooled recalcified citrated human plasma and alpha thrombin were mixed to trigger fibrin formation in microplates and different concentrations of tPA or TNK were evaluated for assay optimization. NTS-105, aprotinin (a serine protease inhibitor serving as control), or DMSO were mixed with human plasma and the fibrinolytic reaction was started by addition of tPA or TNK. Clot formation and lysis were monitored with a spectrophotometer measuring optical density (405 nm) for 180 minutes. The assay results included coagulation and lysis curves, and clot lysis time (CLT) was calculated as the time difference between the maximum fibrin concentration and 50% clot lysis.

**Results:** Complete fibrinolysis was observed with TNK (5.9 µg/mL), and partial fibrinolysis with tPA (0.5 µg/mL). Aprotinin inhibited fibrinolytic activity of tPA and TNK. DMSO increased the fibrinolytic activity of tPA but not TNK. NTS105 at 5 µg/mL had no effect on TNK fibrinolytic activity, and slightly increased tPA fibrinolytic activity.

**Conclusions:** Compound effects on fibrinolysis can be evaluated with the turbidimetric fibrinolytic assay. NTS-105 did not adversely affect TNK fibrinolytic activity and partially increased tPA-induced clot lysis.

## P57 Evaluation of the Translational Relevance of Rat Mammary Tumors to Human Breast Cancer Using Immunophenotypic Characterization

Allison C. Boone<sup>1,2</sup>, Morgan Hernandez<sup>3</sup>, Heather Jensen<sup>2</sup>, David Cunefare<sup>4,2</sup>, Charan Ganta<sup>5,2</sup>, Keith Shockley<sup>6</sup>, Cynthia Rider<sup>2</sup>, Ronald Herbert<sup>2</sup>, Robert Sills<sup>2</sup>, Arun Pandiri<sup>2</sup>

<sup>1</sup>Experimental Pathology Laboratories, Morrisville, NC, USA.

<sup>2</sup>Division of Translational Toxicology, National Institute of Environmental Health Sciences, Research Triangle Park, NC, USA. <sup>3</sup>The University of Texas Permian Basin, Odessa, TX, USA.

<sup>4</sup>Charles River Laboratories, Durham, NC, USA. <sup>5</sup>Inotiv, Morrisville, NC, USA. <sup>6</sup>Division of Intramural Research, National Institute of

Environmental Health Sciences, Research Triangle Park, NC, USA.

### Abstract

**Introduction:** Rat mammary fibroadenomas and adenocarcinomas share several morphologic features with human breast cancer (HBC); however, their immunophenotypic classification and translational relevance are poorly understood. **Experimental Design:** We examined rat mammary tumors using a panel of immunohistochemical (IHC) biomarkers commonly used in HBC diagnosis and prognosis. **Methods:** Harlan Sprague Dawley rat mammary tumors arising spontaneously (adenocarcinoma, n=18) or from chronic inhalation exposure to alpha (α)-pinene (fibroadenoma, n= 38, and adenocarcinoma, n=21) were obtained from the National Toxicology Program archives. IHCs using antibodies against estrogen receptor alpha (ERα), progesterone receptor (PR), HER2/Neu, and Ki67 were performed on all samples. Artificial intelligence-based image analysis (Visiopharm) was performed on whole slide digital scans to quantify positively stained regions of interest. **Results:** There was significant overexpression of HER2/Neu in mammary adenocarcinomas from the α-pinene exposed groups compared to those arising spontaneously. Also, there was significant overexpression of Ki67, HER2/Neu, and PR in the mammary adenocarcinomas compared to the fibroadenomas from the α-pinene exposed groups. **Conclusions:** Significant overexpression of HER2/Neu in mammary adenocarcinomas from α-pinene exposure in comparison to those arising spontaneously suggests that α-pinene exposure may amplify the HER2/Neu signaling network. The significant differences in Ki67, HER2/Neu, and PR expression observed in mammary adenocarcinomas and fibroadenomas from α-pinene exposures may be related to differences in tumor morphology. **Impact Statement:** These data provide a mechanistic insight into rat mammary carcinogenesis as well as help to understand the translational relevance of these rodent tumors to human breast cancer.

## P58 Rodent Tumors from $\alpha$ -Pinene Exposure Harbor Unique Mutation Signatures and Enriched Mutational Motifs

Arun Pandiri<sup>1</sup>, Jianying Li<sup>2</sup>, Ashley Brooks<sup>2</sup>, Dmitry Gordenin<sup>3</sup>, Leszek Klimczak<sup>2</sup>, Ella Gunady<sup>4</sup>, Thai-Vu Ton<sup>1</sup>, Cynthia Rider<sup>5</sup>, Ronald Herbert<sup>1</sup>, Robert Sills<sup>1</sup>, Jian-Liang Li<sup>2</sup>, David Adams<sup>6</sup>  
<sup>1</sup>Comparative and Molecular Pathogenesis Branch, Division of Translational Toxicology, National Institute of Environmental Health Sciences, Research Triangle Park, NC, USA. <sup>2</sup>Biostatistics and Computational Biology Branch, National Institute of Environmental Health Sciences, Research Triangle Park, NC, USA. <sup>3</sup>Genome Integrity and Structural Biology Laboratory, Division of Intramural Research, National Institute of Environmental Health Sciences, Research Triangle Park, NC, USA. <sup>4</sup>Princeton University, Princeton, NJ, USA. <sup>5</sup>Systems Toxicology Branch, Division of Translational Toxicology, National Institute of Environmental Health Sciences, Research Triangle Park, NC, USA. <sup>6</sup>Wellcome Sanger Institute, Cambridge, United Kingdom.

### Abstract

**Background:** The cancer hazards due to  $\alpha$ -pinene, the main component of turpentine, are poorly understood. We have examined the genomic alterations in rodent tumors arising spontaneously or from chronic exposure to  $\alpha$ -pinene.

**Methods:** Whole genome sequencing was performed on rat mammary tumors (rMTs, n=32), mouse hepatocellular carcinomas (mHCCs, n=38) and mouse alveolar/bronchiolar carcinomas (mABCs, n=12). Mutation signatures were compared to the human cancer databases to determine the translational relevance to human cancers. In addition, mutational motif-centered analysis was performed to determine enrichment with a trinucleotide aTn previously associated with mutagenic small epoxides.

**Results:** Chronic  $\alpha$ -pinene inhalation exposure in rats and mice resulted in a dose-dependent increase in tumor mutation burden (mHCCs and rMTs > mABCs).  $\alpha$ -pinene rMTs but not spontaneous rMTs showed unique exposure specific COSMIC signatures (SBS12 and SBS21). Interestingly, the *de novo* signature A in  $\alpha$ -pinene-exposed mHCCs and mABCs showed a comparatively high similarity to SBS118 and SBS161 in the Signal database. Signatures SBS1 and SBS5 associated with aging were reported in most of the rodent tumors examined in this study. Mutational motif analysis revealed an enrichment of aTn to aGn in rMTs and mHCCs but not in mABCs.

**Conclusions:** Significant dose dependent increase of mutation burden as well as enrichment of aTn to aGn motifs in rMTs and mHCCs but not in mABCs support a mutagenic mode of action. The tumor specific differences in mutation signatures and motif enrichments may be related to the different mutagenic processes and/or DNA repair in the respective target organs.

## P59 Spontaneous Neoplasms in the Ovary of Mice from Carcinogenicity Studies

Marcia E. Pereira Bacares, Loudon D. Yantis  
 Labcorp Drug Development, Chantilly, VA, USA.

### Abstract

**Introduction:** Carcinogenicity studies are important in identifying tumorigenic potential in animals as part of the risk assessment for new drugs. Historical control incidences are important considerations when interpreting data and useful when selecting and assessing the suitability of an animal model. This abstract presents and compares the incidence of neoplastic findings in two different mouse models: CD1<sup>®</sup> IGS and CByB6F1-Tg(HRAS)<sup>2</sup>Jic. **Methods:** The incidences of tumors in the ovary were reviewed for 1497 rasH2 control mice (46 studies) and for 594 CD1 control mice (8 studies) conducted at Labcorp Drug Development, Madison between January 1, 2014 and December 31, 2023 (10 years). Neoplasms with incidence rate greater than 1% were considered common, lesser than 1% were considered rare. **Results:** Benign and malignant neoplasms occurred spontaneously in female CD1 and rasH2 transgenic mice. In CD1 mice, common benign tumors included tubulostromal adenoma, cystadenoma, granulosa/theca cell tumor, luteoma, and mixed cell stromal tumor while rare benign neoplasms included adenoma, hemangioma, leiomyoma, and Sertoli cell tumor. Malignant tumors were rare in CD1 and were limited to tubulostromal carcinoma, choriocarcinoma and hemangiosarcoma. In rasH2 transgenic mice, all neoplastic findings were rare and were limited to hemangioma and hemangiosarcoma only. **Conclusion:** Ovarian tumors were more frequent in CD1 with most benign tumors be considered common when compared to rasH2. In rasH2 transgenic mice spontaneous tumors in ovary were considered rare. **Impact statement:** Historical control data help support interpretation of common and uncommon pathology findings and provides a reference for incidence of spontaneous findings.

## P60 Histopathological Characterization of Immune Checkpoint Inhibitor Toxicities in a Humanized Immune System Mouse Model

*Michael J. Goedken*<sup>1</sup>, *Sarah Asby*<sup>2</sup>, *Julie Lang*<sup>2</sup>, *Jordi Lanis*<sup>2</sup>, *Zander Kostka-Newman*<sup>2</sup>, *Kristina Larsen*<sup>2</sup>, *Scott Tilden*<sup>2</sup>, *Roberta Pelanda*<sup>2</sup>, *Xia Wen*<sup>1</sup>, *Lauren M. Aleksunes*<sup>1</sup>, *Melanie S. Joy*<sup>2</sup>

<sup>1</sup>Rutgers University, Piscataway, NJ, USA. <sup>2</sup>University of Colorado, Aurora, CO, USA.

### Abstract

**Introduction:** Immune checkpoint inhibitors (ICIs) have advanced cancer treatment by restoring the ability of the immune system to remove tumor cells. However, prescribing of ICIs can be halted by immune-related adverse events (irAEs). The purpose of this study was to evaluate the ability of a novel tumor-bearing, Human Immune System (HIS) mouse model to recapitulate the histopathological changes associated with ICI-mediated irAEs. **Experimental Design:** Non-humanized BALB/c-Rag2nullIl2rgnullSIRPaNOD (BRGS) and human immune system (HIS-BRGS) mice, humanized with hematopoietic stem cells from human umbilical cord blood, were implanted with MDA-MB-231 triple negative breast cancer cells and treated with vehicle (PBS) or two ICIs (anti-PD-1 nivolumab, anti-CTLA-4 ipilimumab) for 4 weeks prior to histomorphological evaluation of tissues. **Results:** Tumors were larger in vehicle-treated HIS-BRGS compared to BRGS mice. Treatment of HIS-BRGS mice with ICIs reduced tumor weights by 50%. Livers of BRGS mice had healthy parenchyma with occasional tumor cells. By comparison, HIS-BRGS mice exhibited mononuclear cell inflammation that was more severe following ICI treatment. Lungs and kidneys of BRGS mice had no noteworthy findings. However, lungs of ICI-treated HIS-BRGS mice had perivascular mononuclear cell accumulations. Similarly, kidneys of ICI-treated HIS-BRGS mice exhibited minimal-to-mild periarterial accumulations of lymphocytes and multifocal, minimal interstitial mononuclear cell aggregates. No significant findings were observed in skin, heart, muscle, thyroid, or intestines. **Conclusion:** Human Immune System-BRGS mice can be used to evaluate tumor responses to ICI therapies and irAEs in the livers, lungs, and kidneys. **Impact Statement:** Novel preclinical models that capitalize on a humanized immune system can recapitulate clinically-observed ICI toxicities.

## P61 Preclinical Dog Model of Focal Prostate Cancer: Pathology and Novel Theranostics

*Nathan K. Hoggard*<sup>1</sup>, *Gopalakrishnan Ramamurthy*<sup>2</sup>, *Felipe Berg*<sup>2,3</sup>, *Xinning Wang*<sup>2</sup>, *Eric T. Hosnik*<sup>4</sup>, *Matthew Joseph*<sup>4</sup>, *Reena Shakya*<sup>4</sup>, *Dario Palmieri*<sup>4</sup>, *Krishan Kumar*<sup>4</sup>, *Richard M. James*<sup>4</sup>, *Arijit Ghosh*<sup>4</sup>, *Dong Luo*<sup>5</sup>, *Michael V. Knopp*<sup>4</sup>, *Agata A. Exner*<sup>2</sup>, *James P. Basilion*<sup>2</sup>, *Michael F. Tweedle*<sup>4</sup>, *Thomas J. Rosol*<sup>1</sup>

<sup>1</sup>Ohio University, Athens, OH, USA. <sup>2</sup>Case Western Reserve University, Cleveland, OH, USA. <sup>3</sup>Hospital Israelita Albert Einstein, São Paulo, SP, Brazil. <sup>4</sup>The Ohio State University, Columbus, OH, USA. <sup>5</sup>South China University of Technology, Guangzhou, China.

### Abstract

**Introduction:** Dogs develop prostate cancer (PCa) similar to men. We refined a beagle model of PCa using canine Ace-1 cells. The pathology and theranostic (therapeutic-diagnostic) applications are described. **Methods:** Prostates of immunosuppressed, intact, beagle dogs (n=30) were inoculated with Ace-1 cells stably transduced with human gastrin-releasing peptide receptor (hGrPR; n=20), human prostate-specific membrane antigen (hPSMA; n=9), or canine vascular endothelial growth factor A (cVEGFA; n=1). Theranostics were injected into the prostatic artery with fluoroscopic guidance: 1) bombesin peptide analogs (BBN) for hGrPR conjugated with an 800nm near-infrared (NIR) fluorescent dye (n=20) or Lutetium-177-labeled-chelate (n=1) and 2) gold nanoparticles conjugated with a hPSMA ligand and NIR dye (for photodynamic therapy, PDT). All dogs were euthanized 5 weeks after tumor inoculation. Prostate glands and Ace-1<sup>hPSMA</sup> tumors were processed for histopathology, immunohistochemistry, and quantitative PCR. **Results:** The model reliably formed intraprostatic and regionally invasive capsular/intraperitoneal tumors (0.5-2cm). Intraprostatic tumors were within pre-existing glands, had periglandular inflammation, were slow growing, and had low Ki-67 immunolabeling. Regionally invasive tumors grew into and through the capsule, induced granulation tissue, had higher Ki-67 staining (p<0.01), upregulated targetable growth factor receptors (Pdgfra, Slc2a1), and downregulated angiogenesis genes (Vegfa, Vegfc, and their receptors). BBN-NIR perfused the prostate and bound specifically to PCa within 2h. Systemic IV PDT demonstrated internalization of the hPSMA ligand in the tumors. The tumors were treated with a 700 nm laser that induced superficial tumor necrosis. **Conclusion/Impact:** We demonstrated refinement of the dog model of PCa with proof-of-principle for novel therapies/diagnostics.

## P62 Evaluation of the Immune Landscape in a Rat Colon Tumor Model Using Imaging Mass Cytometry

Xuying Zhang<sup>1,2</sup>, Allison Boone<sup>1,3</sup>, Ricardo Cortes<sup>1,3</sup>, Kevin Katen<sup>1</sup>, Carl Bortner<sup>1</sup>, Arun Pandiri<sup>1</sup>

<sup>1</sup>National Institute of Environmental Health Sciences, Research Triangle Park, NC, USA. <sup>2</sup>Gap Solutions Inc., Herndon, VA, USA.

<sup>3</sup>Experimental Pathology Laboratories, Inc., Morrisville, NC, USA.

### Abstract

**Objective:** Spectral overlap associated with fluorescent probes limits the multiplexing capability of immunofluorescence imaging. Imaging Mass Cytometry (IMC) obviates this limitation by using lanthanide metal-tagged antibodies and allows multiplexing of up to 40 targets while providing subcellular resolution and preserving spatial information of the targets. To better understand the spatial immune landscape in the PIRC (polyposis in rat colon) rat colorectal tumors, we have developed a 9 immune cell panel utilizing cytometry by time-of-flight (CyTOF) technology.

**Experimental design:** IMC was used to investigate the expression of immune cell markers in formalin fixed paraffin embedded PIRC rat colorectal tumors (n=10). The 9 immune cell markers included the following targets: T cell types (CD3, CD4, CD8a), B cells (Pax5 and CD20), M1 (CD86) /M2 (CD163) macrophages, as well as programmed cell death-1 (PD-1) and its ligand, programmed cell death-ligand 1 (PD-L1). All candidate antibodies were validated successfully by immunofluorescence staining before their inclusion in the IMC panel.

**Results:** The IMC approach enabled simultaneous identification of different immune cell infiltrates within the rat colorectal tumors.

**Conclusion:** IMC greatly increases the multiplexing capability while preserving the spatial information of the targets. This approach is superior to the classical multiplexed immunofluorescence technique. The IMC panel may be expanded to include biomarkers related to tumor microenvironment and cancer genes.

**Impact statement:** IMC based evaluation of the immune landscape of colorectal tumors in model organisms may help in validating models for immunotherapy.

## P63 INHAND: International Harmonization of Nomenclature and Diagnostic Criteria for Lesions—An Update—2024

Emily K. Meseck<sup>1</sup>, Mark F. Cesta<sup>2</sup>, Victoria Laast<sup>3</sup>, Stacey Fossey<sup>4</sup>, John L. Vahle<sup>5</sup>, Alys Bradley<sup>6</sup>, Matt Jacobsen<sup>7</sup>, Ute Bach<sup>8</sup>, Rupert Kellner<sup>9</sup>, Thomas Nolte<sup>10</sup>, Susanne Rittinghausen<sup>9</sup>, Shim-mo Hayashi<sup>11</sup>, Takanori Harada<sup>12</sup>, Junko Sato<sup>13</sup>, Katsuhiko Yoshizawa<sup>14</sup>

<sup>1</sup>Novartis Pharmaceuticals Corp, East Hanover, NJ, USA. <sup>2</sup>Division of the National Toxicology Program, National Institute of Environmental Health Sciences, Research Triangle Park, NC, USA. <sup>3</sup>Labcorp Early Development, Inc., Madison, WI, USA. <sup>4</sup>Abbvie, North Chicago, IL, USA. <sup>5</sup>Lilly Research Laboratories, Indianapolis, IN, USA. <sup>6</sup>Charles River Laboratories, Trant, Scotland, United Kingdom. <sup>7</sup>Astra Zeneca, Cambridge, United Kingdom. <sup>8</sup>Bayer AG, Wuppertal, Germany. <sup>9</sup>Fraunhofer ITEM, Hannover, Germany. <sup>10</sup>Boehringer Ingelheim Pharma GmbH & Co. KG, Biberach an der Riss, Germany. <sup>11</sup>Tokyo University of Agriculture and Technology, Osaka, Japan. <sup>12</sup>The Institute of Environmental Toxicology, Joso-shi, Ibaraki, Japan. <sup>13</sup>Mediford Corporation, Kamisu-shi, Ibaraki, Japan. <sup>14</sup>Mukogawa Women's University, Nishinomiya, Hyogo, Japan.

### Abstract

The INHAND Proposal (International Harmonization of Nomenclature and Diagnostic Criteria for Lesions in Rats and Mice) has been operational since 2005. A Global Editorial Steering Committee (GESC) coordinates objectives of the project. Development of terminology for rodent organ systems and common non-rodent species used in nonclinical toxicology studies is the responsibility of Working Groups, with experts from North America, Europe, and Japan. All rodent organ systems have been published—Respiratory, Hepatobiliary, Urinary, Nervous Systems, Male Reproductive and Mammary, Zymbals, Clitoral and Preputial Glands and Hematolymphoid System in Toxicologic Pathology and the Integument and Soft Tissue, Female Reproductive System, Digestive System, Cardiovascular System, Skeletal System, Special Senses and Endocrine System in the *Journal of Toxicologic Pathology* as supplements and on a website—[www.goReni.org](http://www.goReni.org), with most recent change control and updates readily available at goRENI.org. Minipig and Dog have been published in *Toxicologic Pathology* in 2021 and Nonhuman primate and Rabbit have been published in the *Journal of Toxicologic Pathology* in 2021. Nonrodent ocular working group manuscript has been submitted to *Toxicologic Pathology* for publication (date pending) and Fish manuscripts will be ready for membership review in 2024. INHAND guides and goRENI.org offer terminology, diagnostic criteria, differential diagnoses, images, and guidelines for recording lesions in nonclinical toxicity and carcinogenicity studies. INHAND GESC representatives work with representatives of US FDA Center for Drug Evaluation and Research (CDER), Clinical Data Interchange Standards Consortium (CDISC), and National Cancer Institute (NCI) Enterprise Vocabulary Services (EVS) to incorporate INHAND terminology as preferred terminology for SEND (Standard for Exchange of Nonclinical Data) submissions to the US FDA. Interest in INHAND nomenclature, based on input from industry and government scientists, is encouraging wide acceptance of this nomenclature.